European Journal of Operational Research 242 (2015) 72–87

Contents lists available at ScienceDirect

European Journal of Operational Research

journal homepage: www.elsevier.com/locate/ejor

Production, Manufacturing and Logistics

Queuing models to analyze dwell-point and cross-aisle location in autonomous vehicle-based warehouse systems

Debjit Roy [a,*], Ananth Krishnamurthy [b], Sunderesh Heragu [c], Charles Malmborg [d]

[a] Production and Quantitative Methods Area, Indian Institute of Management, Ahmedabad, Gujarat 380015, India
[b] Department of Industrial and Systems Engineering, University of Wisconsin-Madison, Madison, WI 53706, USA
[c] School of Industrial Engineering and Management, Oklahoma State University, Stillwater, OK 74078, USA
[d] Department of Industrial and Systems Engineering, Rensselaer Polytechnic Institute, Troy, NY 12180, USA

ARTICLE INFO

Article history:
Received 8 May 2013
Accepted 22 September 2014
Available online 2 October 2014

Keywords:
Logistics
Facilities planning and design
Queuing
Simulation

ABSTRACT

Technological innovations in warehouse automation systems, such as Autonomous Vehicle based Storage and Retrieval System (AVS/RS), are geared towards achieving greater operational efficiency and flexibility that would be necessary in warehouses of the future. AVS/RS relies on autonomous vehicles and lifts for horizontal and vertical transfer of unit-loads respectively. To implement a new technology such as AVS/RS, the choice of a design variable setting, interactions among the design variables, and the design trade-offs need to be well understood. In particular, design decisions such as the choice of vehicle dwell-point and location of cross-aisles could significantly affect the performance of an AVS/RS. Hence, we investigate the effect of these design decisions using customized analytical models based on multi-class semi-open queuing network theory. Numerical studies suggest that the average percentage reduction in storage and retrieval transactions with appropriate choice of dwell-point is about 8 percent and 4 percent respectively. While end of aisle location of the cross-aisle is commonly used in practice, our model suggests that there exists a better cross-aisle location within a tier (about 15 percent from end of aisle); however, the cycle time benefits by choosing the optimal cross-aisle location in comparison to the end of aisle cross-aisle location is marginal. Detailed simulations also indicate that the analytical model yields fairly accurate results.

1. Introduction

To achieve greater operational efficiency and drive competitive advantage, many distribution centers are increasingly interested in adopting automated technologies such as autonomous vehicle-based automated storage and retrieval systems (AVS/RS) for processing unit load transactions in their high density storage areas (Heragu, Cai, Krishnamurthy, & Malmborg, 2008). Savoye Logistics, a France-based equipment manufacturer, pioneered the development of Autonomous Vehicle-based Storage and retrieval system (AVS/RS) (see www.sayove.com). Today, there are more than 35 AVS/RS implementations in Europe and several implementations are currently being planned in USA. Further, several variants of AVS/RS are introduced by Vanderlande Industries and Nedcon.

An AVS/RS consists of autonomous vehicles, lifts, and a rail guide-path within the rack area. The empty or pallet-loaded vehicle navigates along the x-axis (depth of a tier) and the y-axis (width of a tier) using rail guide-paths and travels along the z-axis using lift mechanism. Autonomous vehicles transport pallets along z-axis (vertical direction) between tiers using lifts. A warehouse that uses AVS/RS in the high-density storage area is described in Fig. 1a. A portion of a multi-tier system that illustrates the vehicle-lift interface is depicted in Fig. 1b. Fig. 1c shows a vehicle unloading a pallet on a conveyor roller during the retrieval process. Fig. 2 illustrates the structural components of a multi-tier AVS/RS using a wire-frame model. A multi-tier system is composed of several single tiers. Each tier has a cross-aisle and several aisles. The storage locations, which are single-deep, are located on either side of the aisle. Using a combination of vehicle (horizontal) and lift (vertical) movement, the pallets are being transferred from the load/unload point (LU point) of the first tier to the rack location for processing storage requests or the pallets are being delivered from the rack location to the LU point for processing the retrieval requests.

Conceptualizing system designs using AVS/RS is a prohibitive task because a large number of operational and system design variables, and interactions among them affect the system performance. Design parameters such as location of cross-aisle and depth/width ($\frac{D}{W}$) ratio, vehicle dispatching policy, and dwell-point location have

* Corresponding author. Tel.: +91 7966324823; fax: +91 7966326896.
E-mail address: debjit@iimahd.ernet.in (D. Roy).

http://dx.doi.org/10.1016/j.ejor.2014.09.040
0377-2217/

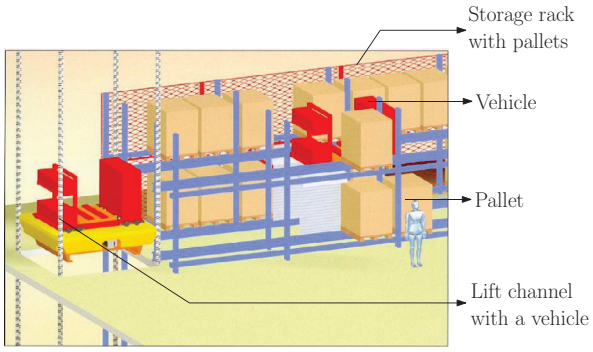

Fig. 1. Illustration of vehicle-lift interface in AVS/RS.

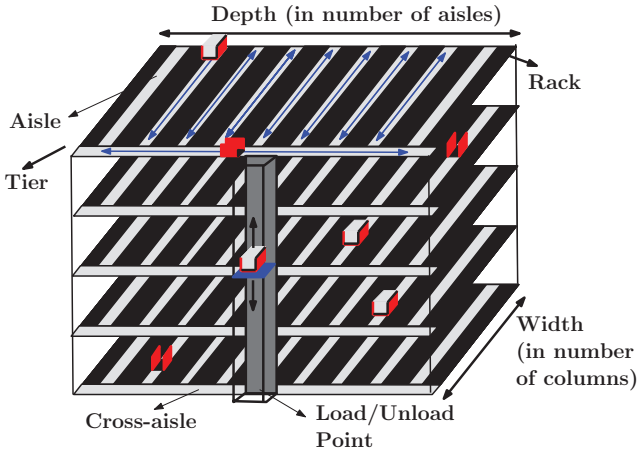

Fig. 2. Wire-frame model of a multi-tier AVS/RS.

performance implications on the system. In practice, the final design is typically obtained after simulating a few configurations in detail and selecting the best among them. The design is improved over time using the performance feedback from live implementations. Therefore, developing analytical models, which can rapidly explore the design space and identify the optimal set of design parameter combinations, can significantly mitigate the risks associated with investments in new technologies. By effectively leveraging advances in automation technology and system design principles, warehouses can achieve greater operational efficiencies.

The initial research focus in AVS/RS was to develop analytical models and obtain aggregate performance measures such as expected throughput times, resource utilization, and expected transaction waiting times (see Malmborg, 2002; Malmborg, 2003; Kuo, Krishnamurthy, & Malmborg, 2007; Fukunari & Malmborg, 2009; Zhang, Krishnamurthy, Malmborg, & Heragu, 2009). In these studies, the emphasis was on understanding the performance of systems with Point of Service Completion (POSC) dwell-point policy and end of aisle location of the cross-aisle.

The dwell-point of a vehicle denotes the location where a vehicle idles after processing a transaction. The choice of a dwell-point policy influences the travel time to process a subsequent transaction. For example, if a vehicle dwells at the point of service completion and the subsequent transaction involves retrieving a pallet from the same aisle, then the POSC dwell-point decision is an efficient choice. However, if the subsequent transaction is a storage transaction then LU dwell-point would have been a better dwell-point choice because the pallet (to be stored) is available at the LU point. Therefore, analytical models can help to arrive at an efficient choice of dwell-point policy.

In AVS/RS, cycle time savings may also be obtained by varying the location of the cross-aisle. The location of the cross-aisle influences the horizontal travel time along the direction of an aisle (y-axis). It is not apparent which location among the three choices: end of the aisle, center of the aisle, or somewhere in between is the best choice to place a cross-aisle. Analytical models can help to arrive at an efficient choice of placing the cross-aisle. Due to high-density storage space and additional cost associated with the placement of multiple cross-aisles, only one cross-aisle design is considered in this research.

Zhang (2008) showed that the travel time due to x- and y-axis movement of a vehicle within tiers is a substantial portion (typically between 25 percent and 45 percent) of the total cycle time. Therefore, this research focuses on optimizing the design policies for a single tier will improve the overall system performance.

First, a queuing model of a single tier is developed with LU dwell-point policy and cross-aisle located at the end of the aisle. This model is a multi-class semi-open queuing network model with class switching. The model precisely captures the transaction wait times at the transaction and vehicle synchronization station. The type of vehicle assigned to a transaction (for instance a vehicle situated in the racks versus a vehicle situated at the LU point) is represented with two classes and the vehicles switch their class using a class-switching rule. The queuing model has a non-product form structure, which would require complex analysis to solve in its original form. Therefore, a novel decomposition based approach is adopted to evaluate the model. A detailed simulation model is built and design of experiments is performed to validate the analytical model. The decomposition-based solution approach provides reasonable accuracy for all practical objectives of performance evaluation for a complex system (such as AVS/RS). This model provides the flexibility to analyze the effect of multiple design parameters. For instance, by altering the service time parameters of the analytical model with LU dwell-point policy, the system performance with varying cross-aisle location is evaluated. Numerical studies are performed to develop design insights.

The rest of this paper is organized as follows. Relevant literature is discussed in Section 2. The system description, design trade-offs, and queuing models to analyze the effect of dwell-point policies are presented in Section 3. Similarly, the queuing model to analyze the effect of cross-aisle location is described in Section 4. The solution approach to evaluate the queuing network models and the expressions to obtain the performance measures are included in Section 5. A detailed simulation model is used to study the efficacy of the analytical model. The model validation results and design insights are discussed in Section 6. The conclusions and possible extensions of this research are summarized in Section 7.

2. Literature review

We study relevant literature in three areas: dwell-point policies, cross-aisle location, and AVS/RS models.

1. *Dwell-point policies:* Design policies such as choice of resource dwell-point have been studied in the context of AS/RS using optimization and probabilistic models. In a typical AS/RS, there are multiple parallel aisles of racks with storage cells, a storage retrieval (S/R) machine for each aisle and a Load/Unload (LU) station at the end of the aisle (see Appendix A for basic differences between an AS/RS and an AVS/RS). Park (1999) showed that LU dwell-point policy is optimal for automated storage/retrieval systems with square-in-time racks and dedicated storage. van den Berg (2002) developed analytical expressions and a search routine for determining the optimal dwell-point in AS/RS with randomized and class-based storage policies. Ventura and Lee (2003) proposed an exact polynomial-time algorithm and illustrated that by placing dwell-points at certain pick-up station locations, the throughput time can be minimized in a unidirectional single-loop Automated Guided Vehicle (AGV) system. Meller and Mungwattana (2005)

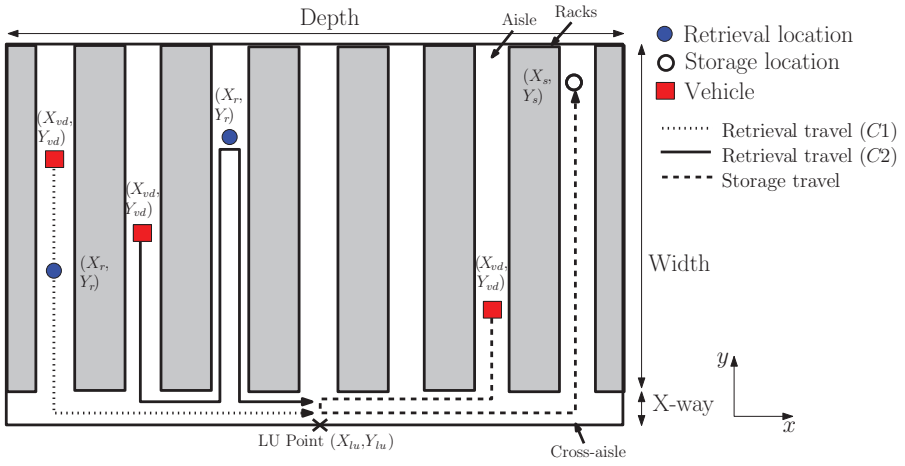

Fig. 3. System description (top view of a single tier).

investigated several dwell-point strategies for an AS/RS through the use of simulation and concluded that the dwell-point strategy has an insignificant impact on the relative system response time when the system is highly utilized. However, these results do not directly apply to AS/RS (see Appendix A for differences in system operations).

2. *Cross-aisle location:* Cross-aisle location has been mainly studied in the context of manual order-pick systems. Vaughan and Petersen (1999) studied the design trade-offs in placing additional cross-aisles in a warehouse and showed that excessive number of cross aisles can actually decrease order picking efficiency. Roodbergen and De Koster (2001) determine order picking routes in a warehouse with two or more cross aisles using multiple heuristics and a branch-and-bound solution algorithm. Ertek, Incel, and Arslan (2007) consider a rectangular warehouse with parallel storage blocks and analyze the effect of placing additional cross-aisles that cut storage blocks perpendicularly and can reduce travel times for picking orders. They determine that equally spaced cross-aisles offer more benefits in comparison to unequally spaced cross-aisles. Berglund and Batta (2012) presented an analytical method for calculating maximally efficient cross-aisle positions subject to a distribution of the storage locations and pick densities in a picker-to-part warehouse. Öztürkoglu, Gue, and Meller (2012) used expected travel time expressions for single command cycles and showed that a chevron arrangement of aisles in a unit-load warehouse is the best design for warehouses with fewer than 27 aisles.
3. *Modeling AVS/RS:* In AVS/RS, several analytical models are developed to study the system performance.
   Malmborg (2002) and Malmborg (2003) developed state equation-based conceptualization models of AVS/R system that provides estimates of cycle time and vehicle utilization. Since solving state equation-based models is computationally expensive, Kuo et al. (2007) used multi-server queuing constructs and presented a computationally efficient nested queuing model to estimate cycle times. In their model, the queuing dynamics between vehicles and transactions is modeled using an $M/G/V$ queue and the dynamics between transactions/vehicles and lift is modeled using a $G/G/L$ queue. Fukunari and Malmborg (2009) develop a queuing network to estimate the performance of AVS/RS with both single and dual command cycle operations. However, the model does not capture the transaction waiting times for availability of a free vehicle. Zhang et al. (2009) also used a multi-server queuing construct to model AVS/RS. However, based on the variation of transaction inter-arrival times, they dynamically selected among three alternative queuing approximations and proposed a procedure for estimating transaction waiting times. Note that the existing models of AVS/RS mainly focus on one particular design configuration with a single LU point and do not explore detailed design trade-offs. Ekren, Heragu, Krishnamurthy, and Malmborg (2010) present a simulation model and use design of experiments to analyze the effect of dwell-point policy, scheduling rule, input/output (I/O) locations and interleaving rule on AVS/RS throughput time performance.
   Recently, Roy, Krishnamurthy, Heragu, and Malmborg (2012) developed an analytical model for conceptualizing AVS/RS design using semi-open queuing network theory. Using the model, they suggested that $\frac{D}{W} = 2$ provides best system performance and multiple horizontal zones of a tier are more beneficial than a single zone. By using the right combination of design parameter settings, the expected transaction cycle times can be reduced up to 25 percent (Roy (2011)).

Our research contributes to the present growing literature in the following ways:

1. We develop new customized queuing network models to analyze the effect of dwell-point policy and location of the cross-aisle on AVS/R system performance.
2. We evaluate the network using a novel decomposition-based approach.
3. By partitioning a tier into multiple regions, we develop probabilistic travel time expressions to analyze varying location of a cross-aisle for different service types.
4. Further, we consider expected transaction waiting times in addition to the expected vehicle travel times to develop insights.

3. Analysis of dwell-point policy

In this section, the design trade-offs are analyzed with respect to LU point dwell-point policy, i.e., the vehicle dwells as the LU point after processing a storage transaction. The system description and the design trade-offs are presented in Section 3.1. The queuing network model, that is developed to analyze the effect of LU point dwell-point policy, is described in Section 3.2.

3.1. System description and assumptions

A tier of a storage area is composed of a set of aisles with storage racks on both sides of each aisle (Fig. 3). A cross-aisle is located

at the end of the tier and it runs orthogonal to the aisles. Vehicles travel between aisles using the cross-aisle. A system of rails guides the rectilinear movement of vehicles along x and y dimensions. The depth of a tier is measured along the cross-aisle (x-axis) whereas the width of the tier is measured from the beginning of the rack to the end of the rack along the aisle (y-axis). The X-way distance denotes the distance from the cross-aisle (x-axis) to the beginning of the racks.

We first describe the processing sequence of storage transaction with a LU dwell-point policy. Note that in LU dwell-point policy, the vehicles dwell/idle at the LU point. There are two possible vehicle statuses that a pallet to be stored finds on arrival: (1) pallet finds an idle vehicle on arrival and (2) pallet does not find any idle vehicle on arrival. If a pallet finds an idle vehicle, the vehicle is assigned to the storage transaction. The vehicle initiates its travel from the dwell-point coordinates (X_{vd}, Y_{vd}), picks the pallet and travels along the cross-aisle and aisle to reach the storage location (X_s, Y_s). If a pallet to be stored does not find a vehicle on arrival, the pallet waits at the LU point to be picked up by the vehicle. Once a free vehicle is available, the transaction claims the vehicle and the vehicle travels to the LU point (X_{lu}, Y_{lu}). Then the vehicle picks the pallet and travels along the cross-aisle and aisle to reach the storage location (X_s, Y_s). The vehicle unloads the pallet at the storage location and dwells/idles. Similarly, depending on the vehicle status, two possibilities arise to process a retrieval transaction. If an idle vehicle is present, then it travels to the retrieval location from the LU point and retrieves the pallet. Then the vehicle travels along the rectilinear path to the LU point and unloads the pallet. If an idle vehicle is not present, the transaction waits in a virtual buffer if a vehicle is unavailable. Once a vehicle is assigned to the transaction, it travels to the retrieval location (X_r, Y_r) and retrieves the pallet to the LU point.

Now we discuss the distinguishing travel movements for processing a transaction using POSC dwell-point policy instead of a LU dwell-point policy. In POSC dwell-point policy, the vehicle dwells/idles at its point of service completion, which is an interior rack location for the case of a storage transaction and LU point for the case of a retrieval transaction. The processing sequences for storage and retrieval transactions with POSC and a LU dwell-point policy are identical for the case when the transaction does not find any idle vehicle on arrival. However, if the transaction finds an idle vehicle on arrival, the processing sequences for storage and retrieval transactions with POSC and a LU dwell-point policy may differ in the initial travel movement. With POSC dwell-point, the vehicle may start its movement from an interior rack location (and not a LU point) where it dwelled after processing a storage transaction. We further compare the two dwell-point policies using cycle time expressions in this section.

The travel paths corresponding to the processing sequences of storage and retrieval transactions are also depicted in Fig. 3. The waiting time for a free vehicle, horizontal travel velocity, load and unload times are denoted by W_V, v_h, L_t, and U_t respectively.

Based on retrieval location, two cases are analyzed to obtain cycle time expressions for retrieval transactions. Case C_1 provides expression for the scenario where the vehicle originates from an interior location in the rack, and the aisle corresponding to the vehicle origin is the same as the aisle corresponding to the retrieval location. Case C_2 corresponds to the other two scenarios of vehicle origin and retrieval location, namely, (1) when vehicle originates from an interior location but the aisle corresponding to the vehicle origin is different from the aisle of retrieval location, and (2) when the vehicle originates from LU point. The above description of system operations yields the expressions for storage and retrieval cycle times (CT_s and CT_r). The expressions corresponding to the two cases are shown as C_1 and C_2 in Eq. (2). The components of the cycle times in Eqs. (1) and (2) correspond to the steps in the processing sequence of storage and retrieval transactions respectively (Roy et al., 2012).

$$CT_s = W_V + \left(\left|\frac{X_{vd} - X_{lu}}{v_h}\right| + \left|\frac{Y_{vd} - Y_{lu}}{v_h}\right|\right) + L_t + \left(\left|\frac{X_{lu} - X_s}{v_h}\right| + \left|\frac{Y_{lu} - Y_s}{v_h}\right|\right) + U_t \quad (1)$$

$$CT_r = \begin{cases} C_1: \; W_V + \left(\left|\frac{Y_{vd} - Y_r}{v_h}\right|\right) + L_t + \left(\left|\frac{Y_r - Y_{lu}}{v_h}\right| + \left|\frac{X_r - X_{lu}}{v_h}\right|\right) + U_t \\ C_2: \; W_V + \left|\frac{Y_{vd} - Y_{lu}}{v_h}\right| + \left(\left|\frac{X_{vd} - X_r}{v_h}\right| + \left|\frac{Y_{lu} - Y_r}{v_h}\right|\right) + L_t \\ \qquad + \left(\left|\frac{Y_r - Y_{lu}}{v_h}\right| + \left|\frac{X_r - X_{lu}}{v_h}\right|\right) + U_t \end{cases} \quad (2)$$

Depending on the storage or retrieval location, either LU dwell-point or POSC dwell-point policy may appear to outperform the other. From cycle time expression for storage transactions (Eq. (1)), LU dwell-point could outperform point of service completion dwell-point policies because the travel time terms $\left|\frac{Y_{vd} - Y_{lu}}{v_h}\right|$ and $\left|\frac{X_{vd} - X_{lu}}{v_h}\right|$ are reduced to zero. However, for retrieval transactions, a POSC dwell-point policy can outperform LU dwell-point policy depending on the dwell-point location and the retrieval location. For instance, when both vehicle and retrieval locations are in the same aisle (Case C_1) for POSC dwell-point, the expression $\left|\frac{Y_{vd} - Y_r}{v_h}\right| + \left|\frac{Y_r - Y_{lu}}{v_h}\right|$ may be greater than or less than the expression $\left|\frac{Y_{lu} - Y_r}{v_h}\right| + \left|\frac{Y_r - Y_{lu}}{v_h}\right|$ for LU dwell-point. Therefore, additional analysis is needed in order to determine which dwell-point policy results in better system performance.

For purpose of analysis, the following assumptions are made.

- The location of the cross-aisle is at the end of the aisle.
- The transactions are processed using single-command cycle only i.e., vehicles process either a storage or a retrieval transaction in one command cycle.
- The horizontal travel velocity for the vehicles is constant; vehicle acceleration/deceleration effects and vehicle turning times are also ignored.
- We ignore the effects of vehicle blocking to decrease model complexity.
- The storage and retrieval transaction arrival process is Poisson.

Additional assumptions and settings of the design parameters (A1–A7) for the queuing network models are summarized in Table 1. A free vehicle is equally likely to be chosen for processing the next transaction. Also the storage and the retrieval locations are uniformly chosen within the tier.

Table 1
Design assumptions for modeling LU dwell-point policy.

Index	Design parameters	Model in Section 3.2
A1	Number of LU points	One
A2	Location of LU points	Middle of cross-aisle
A3	Dwell-point policy	LU
A4	Vehicle assignment rule	Random
A5	Number of zones	One
A6	Storage policy	Uniform
A7	Location of cross-aisle	End of aisle

3.2. Queuing model

The objective of this section is to describe the queuing model developed to study the effect of LU dwell-point policy on system performance. The queuing model for modeling the LU dwell-point policy is described in Fig. 4. There are two types of transactions: storage and retrieval, and V vehicles in the network. To precisely model the effect of LU dwell-point policy on service times, two vehicle classes (i and l) are introduced.

Idle vehicles wait at buffer B_2 in the synchronization station. Storage and retrieval requests wait at buffer B_1 in the synchronization

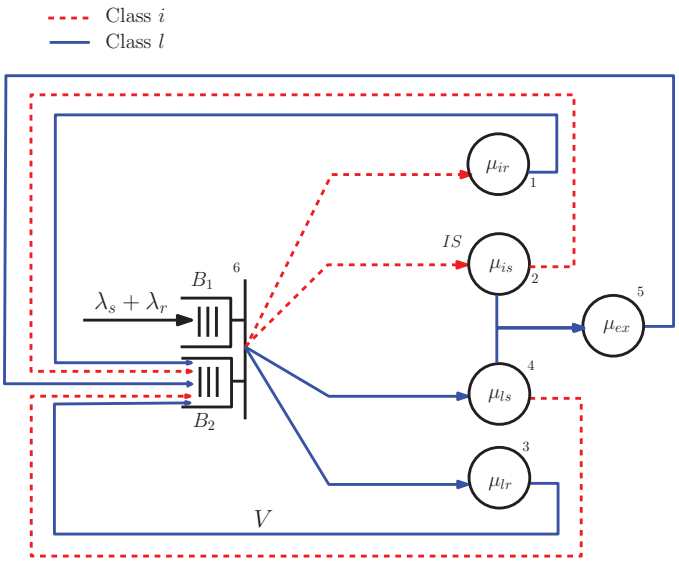

Fig. 4. Queuing network model to analyze LU dwell-point policy.

Table 2
Description of the vehicle class switching rule for LU dwell-point policy.

Vehicle class prior to service	Transaction type	Service type	Condition on y after service	Vehicle class after service
Interior (i)	Retrieval (r)	ir	$y > 0$	Load/unload (l)
Interior (i)	Storage (s)	is	$y > 0$	Interior (i)
Load/unload (l)	Retrieval (r)	lr	$y > 0$	Load/unload (l)
Load/unload (l)	Storage (s)	ls	$y > 0$	Interior (i)
Interior (i)	Retrieval (r)	ir	$y \leq 0$	Load/unload (l)
Interior (i)	Storage (s)	is	$y \leq 0$	Load/unload (l)
Load/unload (l)	Retrieval (r)	lr	$y \leq 0$	Load/unload (l)
Load/unload (l)	Storage (s)	ls	$y \leq 0$	Load/unload (l)

Table 3
Expected service time expressions for LU dwell-point policy.

Expected service time	Expression
μ_{is}^{-1}	$\left(\frac{D'/2+W}{2v_h}\right) + \left(\frac{D'/2+W}{2v_h}\right) + \frac{2x_w}{v_h} + L_t + U_t$
μ_{ir}^{-1}	$\left(\frac{1}{N_a}\right)\left(\frac{W}{3v_h} + \frac{D'/2+W}{2v_h} + \frac{x_w}{v_h}\right)$ $+ \left(\frac{N_a-1}{N_a}\right)\left(\frac{D'/3+W}{v_h} + \frac{D'/2+W}{2v_h} + \frac{3x_w}{v_h}\right) + L_t + U_t$
μ_{ls}^{-1}	$\left(\frac{D'/2+W}{2v_h}\right) + \frac{x_w}{v_h} + L_t + U_t$
μ_{lr}^{-1}	$\left(\frac{D'/2+W}{2v_h}\right) + \left(\frac{D'/2+W}{2v_h}\right) + \frac{2x_w}{v_h} + L_t + U_t$
μ_{ex}^{-1}	$\left(\frac{D'/2+W}{2h_v}\right) + \frac{x_w}{h_v}$

station. To explain the vehicle classes, let us define the term y, which denotes the difference between the number of entities in buffers B_1 and B_2 at any point in time. Therefore, y takes a value between $-V$ and ∞. Then in the network, when $y \leq 0$, there are no transactions in B_1 and vehicles wait at the LU dwell-point for a transaction to arrive. When $y > 0$, there are one or more transactions in B_1 and a vehicle immediately serves another transaction after processing its current transaction. A vehicle that begins its service from the LU dwell-point belongs to l vehicle class whereas a vehicle that begins its service from an aisle location (interior point) belongs to i vehicle class.

As described in this section, corresponding to the two classes of vehicles (i and l), four service types (ir, is, lr, and ls) are defined. Of these, the service types ir and is denote class i vehicle processing retrieval and storage transactions respectively. The service types lr and ls denote class l vehicle processing retrieval and storage transactions respectively. The vehicle switches class potentially after service completion. The vehicle class after servicing a transaction (storage or retrieval) is dependent on value of y at the instant of service completion. For example, after processing a storage transaction, if $y \leq 0$ (i.e., $y \in \{0, -1, -2, \ldots, -V\}$), the class l vehicle retains its class identity l and returns from the aisle storage location to dwell at the LU point. If $y > 0$ at the instant of service completion (indicating waiting transactions i.e., $y \in \{1, 2, \ldots, \infty\}$), then the class l vehicle switches its class identity from l to i and proceeds to process the next transaction in ir or is service type depending on a retrieval or a storage transaction respectively. Similarly, after processing a storage transaction, if $y \leq 0$, a class i vehicle switches its class identity from i to l and proceeds to dwell at the LU point. If $y > 0$ at the instant of service completion (indicating waiting transactions), then the class i vehicle retains its class identity i and proceeds to process the next transaction in ir or is service type depending on a retrieval or a storage transaction respectively. The vehicle classes, transaction types, and service types observed in the system are listed in Table 2.

As seen in Fig. 4, there are six stations in the queuing network. Stations 1–4 represent the four service type nodes, ir, is, lr and ls, and are modeled as infinite server (IS) stations. Station 5 denotes the extra travel required by the i or the l class vehicle to dwell at the LU point after completing a storage transaction. The matching of vehicles and transactions is performed at the synchronization station (node 6). At this node, either transactions wait for a free vehicle in buffer B_1 or vehicles wait for transaction arrivals in buffer B_2. When a transaction and a vehicle are matched together, the vehicle undergoes service in one of the four types (ir, is, lr, or ls). After completing service, the vehicle is released to buffer B_2.

Since the external arrival process of storage and retrieval transactions are assumed to be Poisson with parameters λ_s and λ_r respectively, the interarrival times for the storage and retrieval transactions, X_s and X_r, are exponentially distributed with parameters λ_s and λ_r respectively. The probability of the type of transaction waiting at the head of the queue in buffer B_1 could be storage with probability, $P[X_s < X_r] = \frac{\lambda_s}{\lambda_s+\lambda_r}$ or retrieval with probability $\frac{\lambda_r}{\lambda_s+\lambda_r}$. These probabilities also define the routing probabilities from node 6 to nodes 1–4. The probabilities with which a class i vehicle at B_2 is assigned to process a storage (retrieval) transaction is $\frac{\lambda_s}{\lambda_s+\lambda_r}\left(\frac{\lambda_r}{\lambda_s+\lambda_r}\right)$. Similarly, the probabilities with which a vehicle at a LU point (class l vehicle) can process storage (retrieval) transaction is $\frac{\lambda_s}{\lambda_s+\lambda_r}\left(\frac{\lambda_r}{\lambda_s+\lambda_r}\right)$.

Since the travel times depend on the service type of a vehicle, four travel time expressions that correspond to four service types: ir, is, lr, and ls are needed. The expressions for the expected service time (μ_{ir}^{-1}, μ_{is}^{-1}, μ_{lr}^{-1}, μ_{ls}^{-1}) can be derived based on the system assumptions. The service times are derived in the following subsection.

3.2.1. Service time calculation

In this section, we derive the expression for the expected travel time for service type, ls. When the vehicle dwell-point is LU, the travel time term $\left|\frac{Y_{vd}-Y_{lu}}{v_h}\right|$ reduces to zero. Therefore, for ls service type, the travel time components are: loading the pallet at LU point (L_{vt}), travel time from LU point to storage location $\left(\left|\frac{X_{lu}-X_s}{v_h}\right| + \left|\frac{Y_{lu}-Y_s}{v_h}\right|\right)$, unload time ($U_{vt}$), and travel time from storage location to the LU point $\left(\left|\frac{X_s-X_{lu}}{v_h}\right| + \left|\frac{Y_s-Y_{lu}}{v_h}\right|\right)$. The expected service time for the ls service type can be derived by taking expectation across the travel and load/unload time components (Eq. (3)). The expressions for other service types, which are obtained in a similar fashion, are summarized in Table 3 (refer Appendix B for additional details on the service time expressions). The expression for μ_{ex}^{-1} is equal to $\left(\frac{D'/2+W}{2h_v}\right) + \frac{x_w}{h_v}$.

$$\mu_{ls}^{-1} = E[L_{vt}] + E\left[\left|\frac{X_{lu}-X_s}{v_h}\right|\right] + E\left[\left|\frac{Y_{lu}-Y_s}{v_h}\right|\right] + E[U_{vt}]$$
$$= L_{vt} + \left(\frac{D'/2+W}{2v_h}\right) + U_{vt}$$

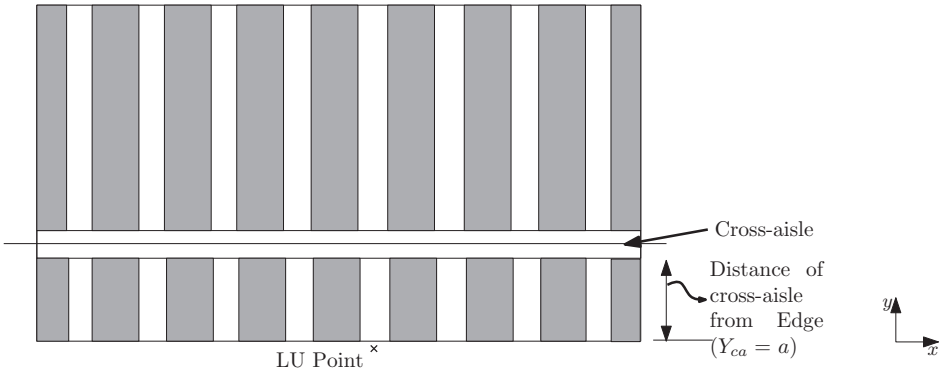

Fig. 5. Top view of a tier with variable cross-aisle location.

Table 4
Design assumptions for modeling variations in cross-aisle location.

Index	Design Parameters	Model in Section 4.2
A1	Number of LU points	One
A2	Location of LU points	End of the main aisle
A3	Dwell-point policy	LU point
A4	Vehicle assignment rule	Random
A5	Number of zones	One
A6	Storage policy	Uniform
A7	Cross-aisle location	Variable

4. Analysis of cross-aisle location

In this section, the effect of varying cross-aisle location on system performance is analyzed. The system description and the design trade-offs are presented in Section 4.1. The queuing network model, that is developed to analyze the effect of cross-aisle location, is described in Section 4.2. Further, the service time calculations for the various service types are explained in Section 4.3.

4.1. System description and assumptions

Recall that a tier of a storage area is composed of a set of aisles with storage racks on both sides of each aisle (Fig. 3). A cross-aisle runs orthogonal to the aisles and in most cases, is located at the end of the aisles. However, in this research, we examine whether other locations of the cross-aisle would be more effective. To do so, a parameter Y_{ca} that denotes the distance of the cross-aisle from the end of the aisle is defined (see Fig. 5). In particular, $Y_{ca} = 0$ indicates that the cross-aisle is located at the end of the aisle and $Y_{ca} = a$ indicates that the cross-aisle is located a units away from the end of the aisle. When the cross-aisle is located at the end of the aisle, the expressions for storage and retrieval cycle times (CT_s and CT_r) are obtained by substituting Y_{ca} in place of Y_{lu} in Eqs. (1) and (2) respectively. From the cycle time equations, it can be seen that $\left|\frac{Y_{vd}-Y_{lu}}{v_h}\right| + \left|\frac{Y_{lu}-Y_r}{v_h}\right|$ may be less than, greater than, or equal to $\left|\frac{Y_{vd}-Y_{ca}}{v_h}\right| + \left|\frac{Y_{ca}-Y_r}{v_h}\right|$ depending on the vehicle dwell-point and location of the cross-aisle. Hence, it is not obvious whether the cross-aisle should be at the end, center or somewhere in between the aisles.

For purpose of analysis, we assume that the vehicle dwells at the LU point i.e., a vehicle that completes a retrieval transaction dwells at the LU point and a vehicle that completes a storage transaction and travels to dwell at the LU dwell-point. Further, the location of the cross-aisle varies along the y-axis. Additional assumptions and settings of the design parameters (A1–A7) for the queuing network models are summarized in Table 4. The queuing model for analyzing the effect of cross-aisle location is presented in the next section.

4.2. Queuing model

The semi-open queuing network model developed for the case of cross-aisle located at the end of the aisle and LU dwell-point policy in Section 3.2 is adapted to analyze the effect of varying cross-aisle location (see Fig. 4). Similar to the model described in Section 3.2, we need two vehicle classes (i and l) and four service types (is, ir, ls, and lr) to model variable cross-aisle location with LU dwell-point policy. The vehicle switches its class based on the class switching rules described in Table 2.

From the cycle time expressions (refer Eqs. (1) and (2)), it can be observed that the travel time components differ with the location of the cross-aisle. Hence, the mean service time expressions at service nodes is, ir, ls, and lr need to be modified. Therefore, new service time expressions for the four service types are developed in the next section.

4.3. Service time calculation

To illustrate the service time variations, six regions are defined (refer Fig. 6). The aisle along the LU point is denoted as a *main aisle* because all vehicles use this aisle to process a transaction. If the number of aisles is an odd number, the main aisle divides the rack into two equal halves. The area of the rack above the cross-aisle is referred as *Upper Portion* (*UP*) whereas the area of the rack below the cross-aisle is referred as *Lower Portion* (*LP*). Based on the location of the LU point and the cross-aisle, the vehicle location ($L_V(r)$) and the transaction (storage/retrieval) location ($L_T(r)$) belong to one of the six regions ($r = 1, \ldots, R$, and $R = 6$): Upper Left (*UL*), Upper Right (*UR*), Lower Left (*LL*), Lower Right (*LR*), Main aisle Upper (*MU*), and Main aisle Lower (*ML*). The areas of the four regions (*UL*, *UR*, *LL*, and *LR*) are defined by the location of the main aisle and cross-aisle. The areas of the four regions are equal only when the cross-aisle is located at the center and the main aisle divides the tier into two equal halves.

To determine the expected service time expressions for four service types (denoted by $\mu_{is}'^{-1}$, $\mu_{ir}'^{-1}$, $\mu_{ls}'^{-1}$, and $\mu_{lr}'^{-1}$), a three-step approach is followed. First, based on the location of the vehicle and transaction, scenarios are developed for each service type. Then, for each scenario, the expected service time is calculated. Finally, the expected time for each service type is obtained by taking an expectation across all scenarios.

Due to symmetry in travel times from a LU point to an interior point and from an interior point to a LU point, the expected travel times for the is and lr, service types are always twice that of expected travel time for the ls service type. Hence, the scenarios used in determining $\mu_{ls}'^{-1}$ are enough to determine $\mu_{is}'^{-1}$ and $\mu_{lr}'^{-1}$. Therefore, the methodology to determine the service time expressions is explained for ls and ir service types only. Note that we distinguish the service

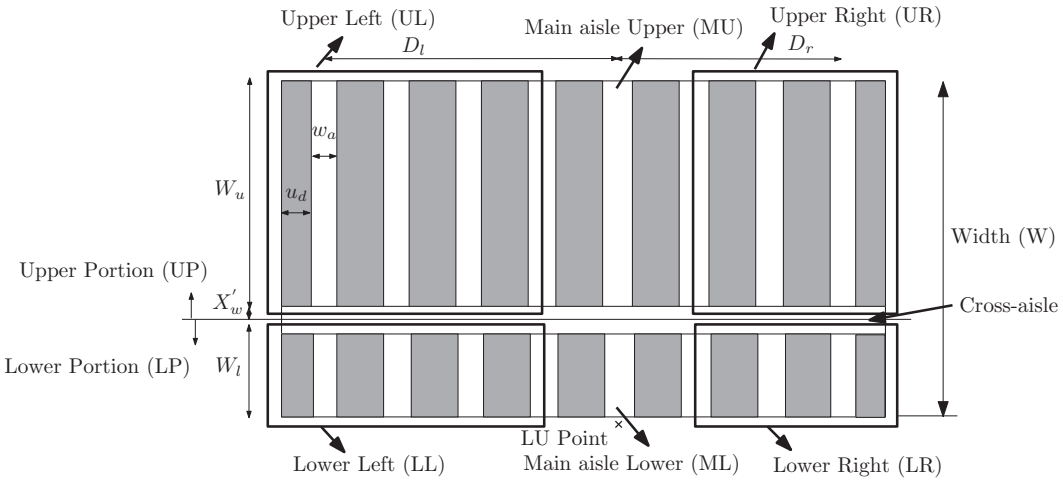

Fig. 6. Regions of a tier with variable cross-aisle location.

time expressions for the cross-aisle variation from the other models by using a superscript, (′).

Expected service time for *ls* service type ($\mu_{ls}^{\prime -1}$): When the vehicle originates from the LU point ($L_V(r) = ML$) to process a storage transaction (*ls* service type), depending on the storage location, six scenarios exist corresponding to the regions ($L_T(r) = UL, UR, LL, LR, MU$, and ML), and are described in Table C.1. The expected travel times for each of these scenarios are derived to determine $\mu_{ls}^{\prime -1}$.

Expected service time for *ir* service type ($\mu_{ir}^{\prime -1}$): Similarly, the expected travel time for the *ir* service type is a function of two location parameters, namely, vehicle location, $L_V(r)$ and transaction (retrieval) location, $L_T(r)$. Based on the location of the LU point and location of the cross-aisle, both vehicle and transaction location ($L_V(r)$ and $L_T(r)$) can belong to one of the six regions: *UL*, *UR*, *LL*, *LR*, *MU*, and *ML*. Therefore, at least 36 service time scenarios are obtained. However, when both vehicle and transaction are located in any of the four areas UL, UR, LL, LR, they may be located either in the same aisle i.e., $L_V(r, j) = L_T(r, j)$ or different aisles i.e., $L_V(r, j) \neq L_T(r, j)$, where j denotes an aisle within a region. Therefore, to account for this possibility, additional four service time scenarios need to be considered. Therefore, to obtain $\mu_{ir}^{\prime -1}$, 40 scenarios need to be considered. Based on the commonality in vehicle and transaction location, these scenarios are grouped into 12 categories (Table C.1). For example, when $L_V(r) = L_T(r) \in \{ML, MU\}$ four scenarios are formed corresponding to $(1)\, L_V(r) = ML, L_T(r) = ML, (2)\, L_V(r) = MU, L_T(r) = MU, (3)\, L_V(r) = MU$, $L_T(r) = ML$, and $(4)\, L_V(r) = ML, L_T(r) = MU$, respectively.

These 46 scenarios are used to determine the expected service time expressions. The notations $t_{m,n}$ and $u_{m,n}$ denote the expected service times for the nth scenario in the mth service time category to estimate $\mu_{ir}^{\prime -1}$ and $\mu_{is}^{\prime -1}$ respectively. In Table C.2, the expected service time expression for each scenario is presented. The notations N_{al}, N_{ar}, N_c, N_{cu}, N_{cl}, D_l, D_r, W_u,W_l, x'_w, u_d, and w_a correspond to the total number of aisles, number of aisles towards the left of the main aisle, number of aisles towards the right of the main aisle, total number of columns, number of columns above the cross-aisle, number of columns below the cross-aisle, depth of the rack towards the left of the LU point, depth of the rack towards the right of the LU point, width of the rack above the cross-aisle, width of the rack below the cross-aisle, X-way distance from cross-aisle to the beginning of the aisle, unit depth of a single-deep rack, and width of an aisle. The expected service time expressions that are developed by combining the expressions from the scenarios are included in Table C.3. The term $N_s(m)$ denotes the number of scenarios corresponding to category m. Since there are 12 service time categories for *ir* service types, the expected travel time for *ir* is determined by taking a sum of expectations over 12 categories and scenarios ($N_s(m)$) for each category. Similarly, the expected travel time for *ls* service type is determined by taking a sum of expectations over five categories and scenarios ($N_s(m)$) for each category. As explained earlier, the expected travel times for *is* and *lr* service types are twice the expected travel times for *ls* service type. Therefore, the travel times for *is* and *lr* service types are obtained by multiplying the expected travel times for *ls* category by a factor of 2. The load and unload times are added to obtain the overall service times for all service types. Additional computational details on the cross-aisle service time expressions are provided in Appendix C.

After obtaining the revised service time expressions, the queuing network models are evaluated using the decomposition-based approach.

5. Solution approach and performance measures

The solution methodology to evaluate the queuing models in Sections 3.2 and 4.2 are described in this section. The solution approach is first described for the model with LU dwell-point policy and variations in the approach are presented for the other models. The performance measures desired from the queuing model, such as the average number of transactions waiting in buffer B_1, vehicle utilization, and average transaction cycle times are estimated using a decomposition-based solution approach.

5.1. Decomposition-based solution approach

We leverage the properties of the queuing model illustrated in Fig. 4 to develop the network solution approach. The network possesses the properties of both open (no restriction on the number of customers in the external queue) and closed queuing network (the number of resources (vehicles) in the network is constant). Hence, we decompose the semi-open network based on the value of the parameter y. When $y \leq 0$, vehicles wait to serve transactions whereas when $y \geq 0$, transactions wait to be served (all vehicles are busy). Using this relationship, the semi-open queuing network is decomposed into a closed queuing network and an open queue corresponding to the cases $y \leq 0$ and $y \geq 0$ respectively. The decomposition approach is composed of three steps: (1) determining the conditional measures for the case $y \leq 0$, (2) determining the conditional measures for the network corresponding to the case $y \geq 0$, and (3) linking the solutions from the steps 1 and 2 and estimating the unconditional measures. The details of these steps are discussed now.

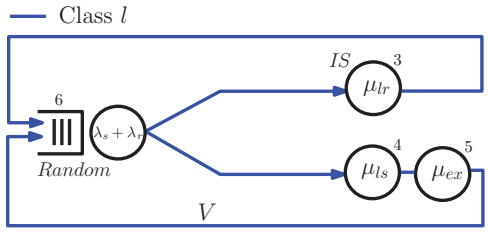

Fig. 7. Closed queuing network for the case $y \leq 0$.

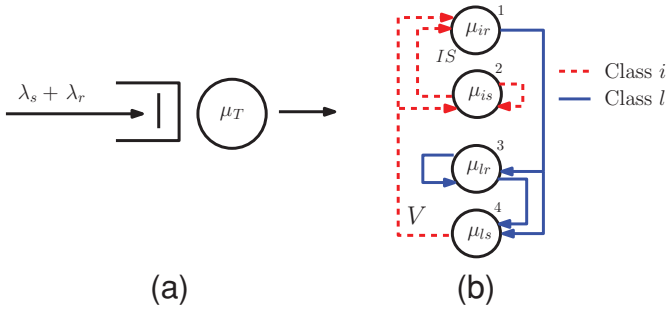

Fig. 8. Illustration of the open queue for the case $y \geq 0$ and closed queuing network for the case $y > 0$

5.1.1. Step 1: Estimating conditional measures from the case $y \leq 0$

When $y \leq 0$, no transactions wait at the external buffer B_1. Since vehicles return to the LU point after processing both types of transactions, this scenario is modeled using a single vehicle class, *l*, and two service types, *lr*, and *ls* (Fig. 7). Vehicle travel times are modeled using Infinite Server (IS) stations (3–5). At node 6, idle vehicles wait for transaction arrivals. Since transactions arrive according to a Poisson process, the service time at this node has an exponential distribution with mean $(\lambda_s + \lambda_r)^{-1}$ and vehicles are assigned to transactions randomly. The distribution of vehicles in the network is captured using a four-tuple state vector, $\mathbf{v}$ where $\mathbf{v} = (v_6, v_3, v_4, v_5)$. The components v_6, v_3, v_4, and v_5 correspond to the number of class *l* idle vehicles at the LU point, the number of busy vehicles whose current service type is *lr*, and *ls*, and the number of vehicles returning to LU point for dwelling respectively.

Since the network is product-form (from BCMP theorem, Baskett, Chandy, Muntz, & Palacios, 1975), the performance of the network can be evaluated using standard solution techniques, convolution algorithm (Buzen, 1973) or mean value analysis (Reiser & Lavenberg, 1980). Using the solution algorithm, the conditional probabilities $(\pi(\mathbf{v}|y \leq 0))$ are obtained at all nodes. The class-specific performance measures are determined using the procedure described in Bolch, Stefan, Meer, and Trivedi (2006).

5.1.2. Step 2: Estimating conditional measures from the case $y \geq 0$

When $y \geq 0$, transactions wait for vehicles to obtain service and all vehicles continuously serve transactions. Hence, this transaction wait phenomena is modeled using a combination of an open queue (transaction wait queue, case $y \geq 0$) and a closed queuing network (vehicle processing network, case $y > 0$).

When $y \geq 0$, there are no free vehicles in buffer B_2. Therefore, an arriving transaction picks up the first available vehicle. The solution to the case $y \geq 0$ is common across any vehicle dwell-point policy. In this case, the open queue has a single server station with a service time denoting the wait time to obtain a free vehicle. Note that the distributions of the service times are unknown. Let us denote the mean service time at this station by the term μ_T^{-1}. Storage and retrieval transactions arrive according to Poisson process with rate λ_s and λ_r respectively (Fig. 8a).

The vehicle processing network is a closed queuing network, which is different than the closed queuing network illustrated in Fig. 7. First, the wait for transaction node (node 6) is not present in this network because vehicles continuously process transactions. Second, the vehicles never dwell. The origin of the vehicles to process transactions is either interior point or LU point. The state of this network is described in terms of the four-tuple state space vector $\hat{\mathbf{v}}$ where $\hat{\mathbf{v}} = (v_1, v_2, v_3, v_4)$ correspond to the number of busy vehicles whose current service type is *ir*, *is*, *lr*, and *ls* respectively. The queuing network is solved using the convolution algorithm and the conditional probabilities $\pi(\hat{\mathbf{v}}|y > 0)$ at all nodes in Fig. 8b are obtained. The distribution of the busy vehicles in the network corresponds to the fraction of the *V* vehicles currently involved in *ls*, *lr*, *is*, and *ir* types of service respectively. After processing a storage transaction in service type *ls*, the vehicle begins to process a transaction waiting at the head of the queue (storage or retrieval) and undergoes service of type *is* or *ir*. The throughput of this queuing network provides an estimate of the average wait time to obtain a free vehicle (the value for μ_T).

Since additional moments of the service time distribution cannot be determined directly by analyzing the closed queuing network in Fig. 8b, we rely on preliminary simulation experiments to analyze the second moment of the inter-departure times from the closed queuing network. By modeling the open queue as an $M/D/1$ queue, we obtain fairly robust and accurate performance estimates (Roy, 2011).

In this step we obtain the following information: (1) the conditional distribution of the average number of vehicles in the closed queuing network when all vehicles are busy $(y > 0)$, and (2) the conditional mean queue length and steady state probability $(\pi(j|y \geq 0))$ of *j* transactions in the queue shown in Fig. 8a (and hence buffer B_2) using Pollaczek–Khinchin mean queue length and LS transform formulas respectively (Gross, Shortle, Thompson, & Harris, 2008).

5.1.3. Step 3: Obtaining unconditional network performance measures

Analyses for case $y \leq 0$ and case $y \geq 0$ provide the conditional distributions for vehicles and transactions in the network when at least one of the two buffers B_1 and B_2 is empty. Let $\pi(y = j), j = 0, \ldots, \infty$ denote the probability of having *j* transactions at buffer B_1, and $\pi(y = j), j = 0, \ldots, -V$ denote the unconditional probabilities of having $|j|$ vehicles at buffer B_2. These probabilities are determined using the law of total probability and the fact that the state $y = 0$ is common to the conditional analysis in both analyses. Recognizing that $\pi(y = 0)$ is common, the following expression can be obtained:

$$\pi(y = 0) = \pi(0|y \geq 0)\pi(y \geq 0) = \sum_{v_1+v_2=0} (\pi(\mathbf{v}|y \leq 0))\,\pi(y \leq 0) \tag{3}$$

The two unknowns in Eq. (3) are $\pi(y \geq 0)$ and $\pi(y \leq 0)$. These two unknowns are obtained as follows. First, it is noted that $\pi(y = 0|y \geq 0)$ is equal to $1 - \rho$, where $\rho = (\lambda_s + \lambda_r)/\mu_T$ is the utilization of the $M/D/1$ queue. Therefore, Eq. (4) is obtained by substituting $1 - \rho$ for the term $\pi(0|y \geq 0)$ in Eq. (3).

$$(1 - \rho)\pi(y \geq 0) = \sum_{v_1+v_2=0} (\pi(\mathbf{v}|y \leq 0))\,\pi(y \leq 0) \tag{4}$$

Further, due to the law of total probability, the following holds:

$$\sum_{j=-V}^{\infty} \pi(y = j) = 1 \tag{5}$$

Eqs. (4) and (5) are solved to obtain the two unknowns $\pi(y \leq 0)$ and $\pi(y \geq 0)$. Knowing $\pi(y \leq 0)$ and $\pi(y \geq 0)$, $\pi(y = j)$ for the case $y \leq 0$ and $y \geq 0$ are determined from Eqs. (6) and (7). When $y \leq 0$, this yields

$$\pi(y = j) = \sum_{v_1+v_2=-j} (\pi(\mathbf{v}|y \leq 0))\,\pi(y \leq 0) \text{ for } j = 0, \ldots, -V. \tag{6}$$

Table 5
Design of experiments for model validation (input).

Model in	$\frac{D}{W}$	$\lambda_s + \lambda_r$ Pallets (hours)	V	U_V (percent)	Number of storage locations	Number of cases
Section 3.2	0.5,1.5	55–135	3, 5	60–90	7290	24
Section 4.2	0.5,1.5	55–165	3, 5	60–90	7290	24

Table 6
Design of experiments for model validation (output).

Model in	Average percent error				Range percent Error			
	$E[CT_r]$ (percent)	$E[CT_s]$ (percent)	U_V (percent)	Q_{B1} (percent)	$E[CT_r]$ (percent)	$E[CT_s]$ (percent)	U_V (percent)	Q_{B1} (percent)
Section 3.2	2.9	3.8	0.9	7.3	−5.8 to 6.0	−8.8 to 9.2	−1.7 to 1.1	−15.1 to 15.8
Section 4.2	2.3	2.7	0.1	7.2	−1.1 to 12.5	−1.2 to 14.0	−0.1 to 1.4	−3.2 to 16.7

and when $y \geq 0$, this yields

$$\pi(y = j) = \pi(j|y \geq 0)\pi(y \geq 0) \text{ for } j = 0, \ldots, \infty. \quad (7)$$

Solving Eqs. (6) and (7), the unconditional steady state distributions and all key performance measures such as the vehicle utilization, distribution of idle vehicles, and average number of vehicles (transactions) waiting for transactions (vehicles) and other performance measures are determined as follows.

Average vehicle utilization (U_V): This metric is determined using the expected number of idle vehicles present at the LU point (Eq. (8)).

$$U_V = 1 - \frac{(Q_l)}{V} \quad (8)$$

Expected storage and retrieval cycle times ($E[CT_s]$ and $E[CT_r]$): Since we have estimated the expected queue length at all stations in the network, the cycle times are calculated using Little's law formula (Eqs. (9) and (10)). The queue length at the external buffer B_1 provides the average wait time to obtain a free vehicle whereas the second term is the average transaction processing time. These two quantities correspond to the waiting time component (W_V), and travel and loading/unloading time components in Eqs. (1) and (2) respectively.

$$E[CT_s] = \frac{Q_{B1}}{\lambda_s + \lambda_r} + \frac{Q_{ls} + Q_{is}}{\lambda_s} \quad (9)$$

$$E[CT_r] = \frac{Q_{B1}}{\lambda_s + \lambda_r} + \frac{Q_{lr} + Q_{ir}}{\lambda_r} \quad (10)$$

The probability distribution of the vehicles ($\pi(\mathbf{v}|y \leq 0)$ and $\pi(\hat{\mathbf{v}}|y > 0)$) can be used to determine the average number of vehicles idle at the LU point (Q_l) and at an interior point (Q_i), and the average number of vehicles processing storage (Q_{is}, Q_{ls}) and retrieval (Q_{ir}, Q_{lr}) transactions in the system. For instance, the terms, Q_l and Q_{lr} are estimated using Eqs. (11) and (12).

$$Q_l = \sum_{(\mathbf{v}:v_6>0)} v_6 \pi(\mathbf{v}|y \leq 0)\pi(y \leq 0) \quad (11)$$

$$Q_{lr} = \sum_{(\mathbf{v}:v_3>0)} v_3 \pi(\mathbf{v}|y \leq 0)\pi(y \leq 0) + \rho \sum_{(\hat{\mathbf{v}}:v_3>0)} v_3 \pi(\hat{\mathbf{v}}|y > 0)\pi(y \geq 0) \quad (12)$$

Average number of transactions waiting for service (Q_{B1}): This measure is given by $(Q_{B1}|y \geq 0)\pi(y \geq 0)$ where $(Q_{B1}|y \geq 0)$ is the average number of transactions waiting when $y \geq 0$ and is determined using Pollaczek–Khinchin mean queue length formula for the $M/D/1$ queue described in Section 5.1.2. The final expression for Q_{B1} is given by Eq. (13).

$$Q_{B1} = \left(\rho + \frac{\rho^2}{2(1-\rho)}\right)\pi(y \geq 0) \quad (13)$$

The semi-open queuing network model developed for understanding the effects of varying cross-aisle location is also solved using the decomposition-based approach with appropriate service time expressions.

6. Design insights from numerical experiments

The results from the analytical model are validated using detailed simulations. The simulation model is built using AutoMod© software v12.2.1 (*www.automod.com*). For each scenario, 15 replications are run with a warmup period of 120 hours and a run time of 600 hours (6000–258,000 transactions). The warmup period eliminates any initial bias due to system startup conditions such as the starting location of the vehicles and initial filled storage locations.

To validate the models in Sections 3.2 and 4.2, the $\frac{D}{W}$ ratio is set at two levels: 0.5 and 1.5; the number of storage locations is set at two levels: 4000 and 7290; and the number of vehicles is varied at two levels: 3 and 5. A summary of the input parameters for the design of experiments is presented in Table 5.

The average absolute error percentages for the performance measures: retrieval cycle time, storage cycle time, vehicle utilization and number of transactions waiting are determined by the expression $(\left|\frac{A-S}{S}\right| \times 100)$, where A and S correspond to the estimate of the measures obtained from analytical and simulation model respectively. The range and average absolute error percentage for the four measures of interest: vehicle utilization, expected transaction cycle time (storage and retrieval), and average number of transactions waiting to be served, are summarized in Table 6. The average absolute percentage errors for utilization and cycle times are less than 3 percent, but the average absolute percentage errors for the number of transactions waiting for free vehicles are a bit higher (up to 8 percent).

We now describe the design insights obtained from numerical experiments. The effects of design parameters are illustrated for a single tier of a warehouse with 7290 locations. In order to understand the interaction between $\frac{D}{W}$ ratio and the design parameters of interest, tiers with two different $\frac{D}{W}$ ratio (1.5 and 0.5) are studied (45 aisles, 81 columns and 27 aisles, 135 columns). The depth, width and X-way distance from cross-aisle to aisle of the tier are 614.64 feet, 437.4 feet and 14 feet respectively. The load and unload times are 15 seconds each. Effects of design parameters on system performance are discussed for cross-aisle location and dwell-point policy.

Dwell-point policy implications: From the numerical experiments performed with two tier configurations ($\frac{D}{W} = 1.5$ and $\frac{D}{W} = 0.5$) and five vehicles, several insights are developed (Fig. 9). In the figure, the y-axis denotes the percentage reduction in expected retrieval and storage cycle times by using LU dwell-point policy over POSC dwell-point policy (Eqs. (14) and (15)). To compare the performance with POSC policy, we leverage the model developed in our previous work

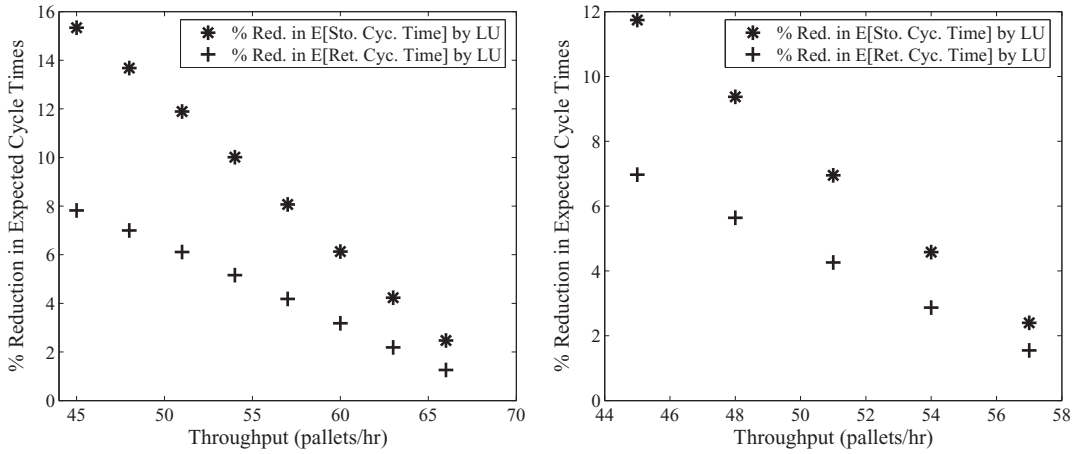

Fig. 9. Effect of dwell-point policies on system performance for $\frac{D}{W} = 1.5$ (left) and $\frac{D}{W} = 0.5$ (right).

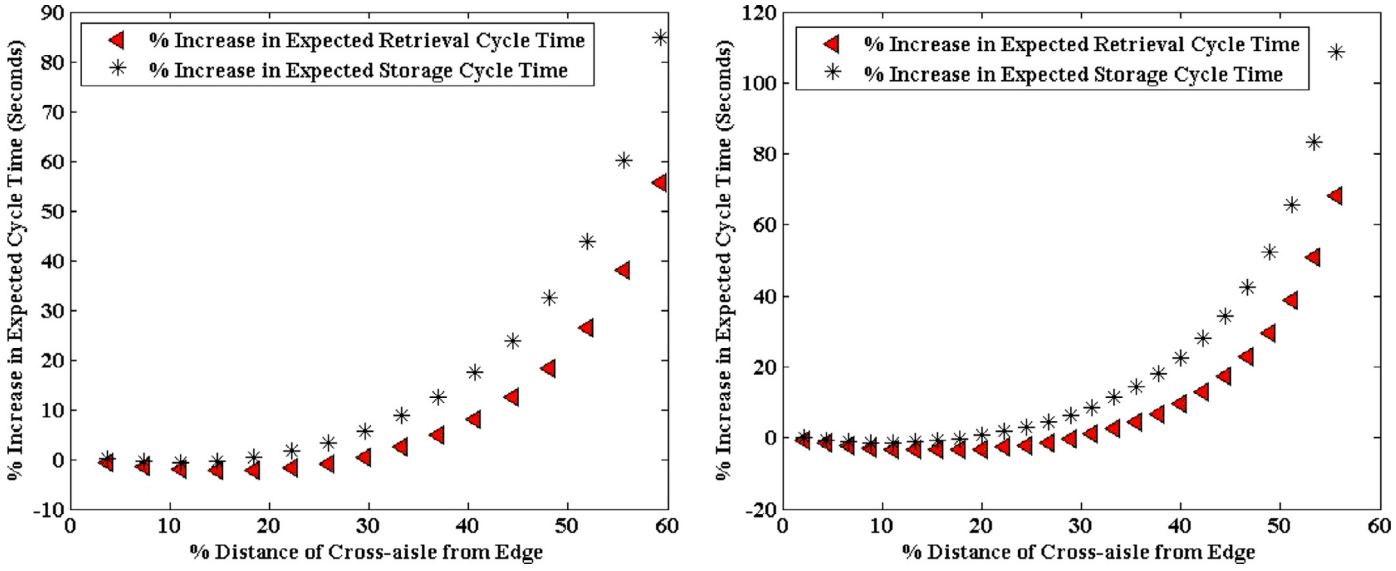

Fig. 10. Percentage increase in cycle times with varying cross-aisle location for $\frac{D}{W} = 1.5$ (left) and $\frac{D}{W} = 0.5$ (right) and LU dwell-point policy.

(see Roy et al. (2012)).

$$\text{Percentage reduction } E[CT_r] = \left|\frac{E[CT_r](\text{LU}) - E[CT_r](\text{POSC})}{E[CT_r](\text{POSC})}\right| \times 100 \text{ percent} \quad (14)$$

$$\text{Percentage reduction } E[CT_s] = \left|\frac{E[CT_s](\text{LU}) - E[CT_s](\text{POSC})}{E[CT_s](\text{POSC})}\right| \times 100 \text{ percent} \quad (15)$$

First, it can be concluded that LU dwell-point policy outperforms POSC dwell-point policy. Greater the $\frac{D}{W}$ ratio, greater is the distance traveled along the cross-aisle path to serve a transaction. By using LU dwell-point policy, the vehicle travels to a LU point. For processing a subsequent transaction (storage or retrieval), the expected vehicle travel time is $\mu_{lr}'^{-1}$ or $\mu_{ls}'^{-1}$. Since, $\mu_{lr}'^{-1} < \mu_{ir}'^{-1}$ and $\mu_{ls}'^{-1} < \mu_{is}'^{-1}$, LU outperforms POSC policy. Third, as vehicle utilization increases, the effect of LU dwell-point policy on system performance diminishes. As vehicle utilizations increase, vehicles have less opportunity to dwell. At very high utilizations, vehicles do not have an opportunity to dwell. Therefore, the effect of dwell policies is not significant.

In the four tier configurations studied in this research, the percentage reduction in storage cycle times with LU dwell-point policy is about twice the percentage reduction in retrieval cycle times with LU dwell-point policy. It is expected that storage transactions will benefit the most using LU dwell-point policy because the pallet is loaded from the LU point only. For storage transactions, the maximum percentage reduction is about 16 percent while the minimum percentage reduction is about 2 percent (at high throughput levels). However, for retrieval transactions, the maximum percentage reduction is about 8 percent while the minimum percentage reduction is about 1 percent.

Cross-aisle location: The location of the cross-aisle is shifted in increments of three columns from the end of aisle and the system performance is evaluated. Tier configurations ($\frac{D}{W} = 1.5$ and $\frac{D}{W} = 0.5$) with five vehicles are used to study the effect of varying cross-aisle location on system performance. Figs. 10 and 11 show the percentage increase in transaction cycle times when the position of the cross-aisle is varied from the end of the aisle location for LU and POSC dwell-point respectively. Results shown in Fig. 10 indicate that as the distance of the cross-aisle from the end of aisle increases, the cycle time improves marginally till a certain point (~15 percent from end of aisle) and then deteriorates. Cross-aisle location at the end of aisle is an efficient choice if not optimal.

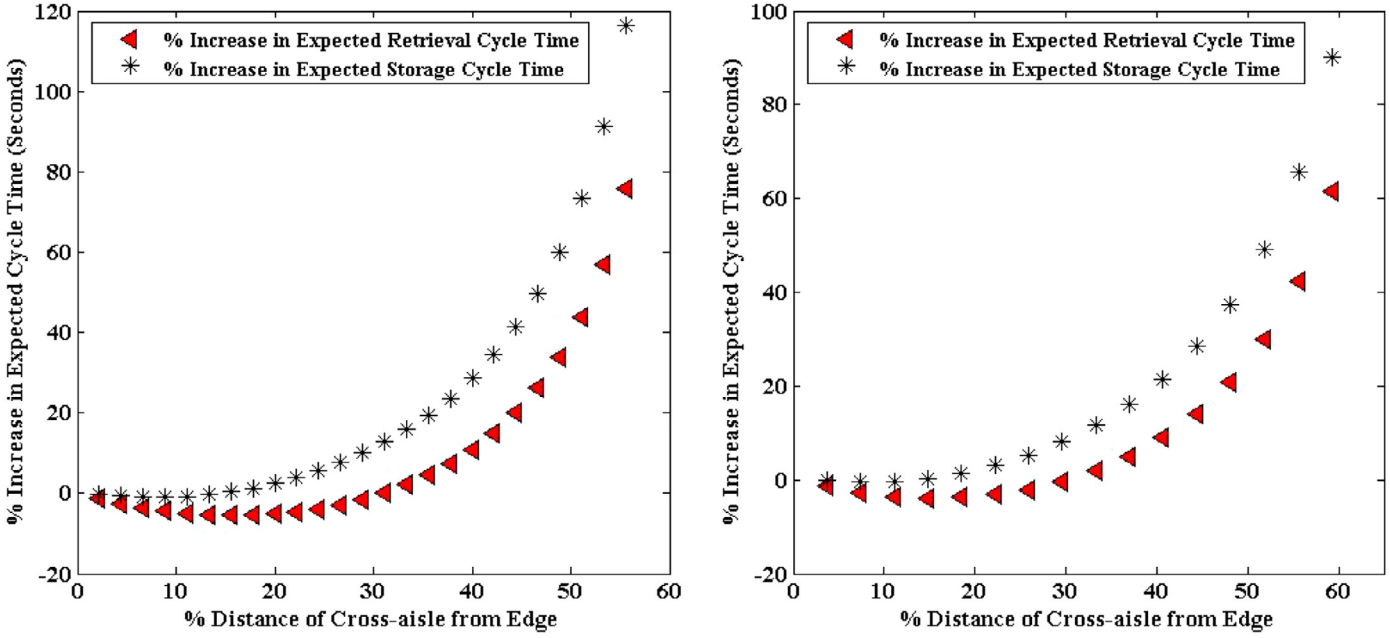

Fig. 11. Percentage increase in cycle times with varying cross-aisle location for $\frac{D}{W} = 1.5$ (left) and $\frac{D}{W} = 0.5$ (right) and POSC dwell-point policy.

7. Conclusions

This paper proposes customized semi-open queuing network models for performance analysis of AVS/RS with varying cross-aisle location and dwell-point policies. The queuing modeling framework precisely captures the effects of dwell-point policy and varying cross-aisle location via vehicle class definition and the travel time expressions at the service nodes. Hence, this general model serves as a building block for analyzing the performance of several AVS/RS configurations. The model is applied to analyze several tier configurations with a combination of design parameters. Analysis results show that end of aisle location of the cross-aisle is an efficient choice and the LU dwell-point policy significantly improves the system performance. This model can be extended to answer other design questions such as the implications of having two or more cross-aisles on system performances, interactions between type of command cycle and layout of warehouse. Further, blocking effects may be dominant in a system with large number of vehicles. The interaction of the dwell-point and cross-aisle location considering blocking effects is subject for future research work.

Acknowledgements

This work is supported in part by the National Science Foundation under grant numbers CMMI-0848756 and CMMI-0946706. We thank the reviewers for their feedback that substantially helped us to improve the paper.

Appendix A. Comparison of AS/RS and AVS/RS

A system view of warehouses that are operated using AVS/RS and AS/RS are shown in Figs. A.1a and b respectively. A typical AS/RS consists of multiple parallel aisles of racks with storage cells, a storage retrieval (S/R) machine for each aisle and an Load/Unload (LU) station at the end of the aisle. The load and unload station could be located either at opposite ends of the aisle or at one end of the aisle. S/R machines are usually stacker cranes which are aisle-captive (Fig. A.1). Common types of AS/RS are mini-load AS/RS, unit-load AS/RS and man-aboard AS/RS.

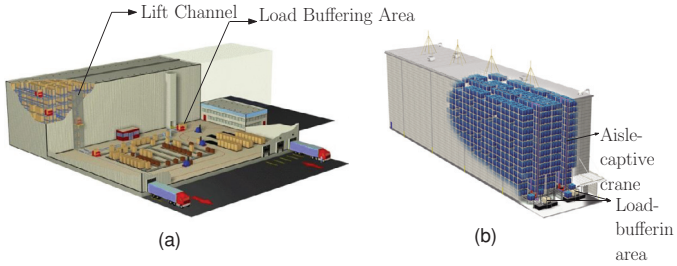

Fig. A.1. Illustration of (a) an AVS/RS operated warehouse (Source: Savoye Logistics), and (b) an AS/RS operated warehouse (Source: Daifuku Material Handling).

Table A.1
Comparison of features between AS/RS and AVS/RS.

Category	AS/RS	AVS/RS
Physical configuration	One LU point per aisle, Conveyors and aisle-captive cranes as S/R devices	One LU point per zone Vehicles and lifts as S/R devices
Load movement	Tchebychev	Rectilinear
Load buffering (area)	One per aisle	One per zone
System throughput	Determined by capacity of crane per aisle and number of aisles	Determined by number of vehicles and lifts

Incoming loads are transported by an accumulating conveyor, which is located at the periphery of the rack system, to the load buffering area (LU station) of the designated aisle. An S/R machine picks the load from the LU station and travels to the designated storage cell location using a Tchebychev movement. This movement increases the travel efficiency due to simultaneous travel along the x and y axes. Similarly, after retrieving the loads, they are deposited at the load buffering area corresponding to the retrieval aisle. From the load buffering area, the load is transferred by the conveyor to the staging area for subsequent operation.

The most significant difference between AS/RS and AVS/RS lies in their physical configuration, load movement process, load buffering process, and system throughput capability. A summary of the comparison between AS/RS and AVS/RS is presented in Table A.1.

Hence, new studies are needed to understand design-tradeoffs in AVS/RS.

Appendix B. Service time expressions for LU dwell-point policy

Service time calculation for LU dwell-point policy

In this section, we explain the expression for the expected travel time for the four service types (shown in Table 3). Note that in the *ls* service type, the vehicle originates from the LU dwell-point to process the storage transaction. We capture the expected travel time for the travel including the pallet loading and unloading times in μ_{ls}^{-1}. The expected travel time to reach the storage location along the aisle and cross-aisle is given by $\left(\frac{D'/2+W}{2v_h}\right)$. The deterministic travel time on the X-way is given by $\frac{x_w}{v_h}$. The expected travel times along with the deterministic loading and unloading times provides the expression for μ_{ls}^{-1}. However, after processing the storage transaction, the vehicle returns back to the LU point to dwell if there are no transactions waiting to be served. The expected travel time to reach the LU point from the storage location along the aisle and cross-aisle, μ_{ex}^{-1} is given by $\left(\frac{D'/2+W}{2v_h}\right) + \frac{x_w}{v_h}$.

Likewise, in the *lr* service type, the vehicle originates from the LU dwell-point to process a retrieval request. So the vehicle first travels along the cross-aisle and the aisle (the expected travel time given by $\left(\frac{D'/2+W}{2v_h} + \frac{x_w}{v_h}\right)$. Then the vehicle picks the pallet, and returns to unload the pallet at the LU point using the aisle and cross-aisle path (the expected travel time for this segment of the activity along with the deterministic loading and unloading times is given by $\left(\frac{D'/2+W}{2v_h} + \frac{x_w}{v_h} + L_{vt} + U_{vt}\right)$.

In the *is* service type, the vehicle starts processing the storage request from an interior location (within the racks). The vehicle first travels to the LU point to pick the pallet. The expected travel time for this segment is given by $\left(\frac{D'/2+W}{2v_h}\right) + \frac{2x_w}{v_h}$. After picking the pallet, the vehicle travels to the storage location and unloads the pallet. This expected travel time along with load/unload times is given by $\left(\frac{D'/2+W}{2v_h} + \frac{2x_w}{v_h} + L_t + U_t\right)$. Similar to *ls* service type, after processing the storage transaction, the vehicle returns back to the LU point to dwell if there are no transactions waiting to be served; the expected travel time for the dwell-point travel is indicated by μ_{ex}^{-1}.

In the *ir* service type, the vehicle originates from the interior point to process a retrieval transaction. The vehicle could be present in the same aisle from where the load needs to be retrieved or it could be in a different aisle. So we determine the conditional expected travel times for the two possibilities and then determine the unconditional service time. In the first case, the vehicle is present in the same aisle from which the load needs to be retrieved. The expected travel time to reach the load retrieval location ($\frac{W}{3v_h}$), then the time to pick the pallet and expected travel time to reach the LU point using the aisle and cross-aisle path is given by $\left(\frac{D'/2+W}{2v_h} + \frac{x_w}{v_h} + L_t + U_t\right)$. Hence, the vehicle needs to retrieve the pallet from another aisle. Hence, the vehicle first reaches the destination aisle and retrieval location $\left(\frac{D'}{3v_h} + \frac{W}{v_h}\right)$. Then the vehicle travels within the destination aisle to retrieve the pallet, and uses the aisle and cross-aisle to reach the LU point and unload the pallet $\left(\frac{D'/2+W}{v_h} + \frac{2x_w}{v_h} + L_t + U_t\right)$.

Appendix C. Service time computation for different cross-aisle locations

We first list the 12 scenarios (that contains 40 sub-scenarios), which are developed to estimate the travel time for the *ir* service type. Then, we list the six subscenarios developed to estimate the travel times for the *is*, *lr*, and *ls* service types (see Table C.1). As discussed in the main text, $L_V(r)$ and $L_T(r)$ denote the location of the vehicle and the retrieval location of the pallet respectively.

Table C.1
Scenarios for service time computation for different cross-aisle locations.

Expected service time	Category description (m)	Scenario description (n)
$\mu_{ir}^{'-1}$	(1) $L_V(r) = L_T(r) \in \{ML, MU\}$	(1) $L_V(r) = ML, L_T(r) = ML$ (2) $L_V(r) = MU, L_T(r) = MU$ (3) $L_V(r) = MU, L_T(r) = ML$ (4) $L_V(r) = ML, L_T(r) = MU$
	(2) $L_V(r) = L_T(r) \notin \{ML, MU\}$	(1) $L_V(r) = UL, L_T(r) = UL$ (2) $L_V(r) = LL, L_T(r) = LL$ (3) $L_V(r) = UR, L_T(r) = UR$ (4) $L_V(r) = LR, L_T(r) = LR$
	(3) $L_V(r) = UL, L_T(r) = LP$	(1) $L_V(r) = UL, L_T(r) = LL$ (2) $L_V(r) = UL, L_T(r) = ML$ (3) $L_V(r) = UL, L_T(r) = LR$
	(4) $L_V(r) = UR, L_T(r) = LP$	(1) $L_V(r) = UR, L_T(r) = LR$ (2) $L_V(r) = UR, L_T(r) = ML$ (3) $L_V(r) = UR, L_T(r) = LL$
	(5) $L_V(r) = LL, L_T(r) = UP$	(1) $L_V(r) = LL, L_T(r) = UL$ (2) $L_V(r) = LL, L_T(r) = MU$ (3) $L_V(r) = LL, L_T(r) = UR$
	(6) $L_V(r) = LR, L_T(r) = UP$	(1) $L_V(r) = LR, L_T(r) = UR$ (2) $L_V(r) = LR, L_T(r) = MU$ (3) $L_V(r) = LR, L_T(r) = UL$
	(7) $L_V(r) = LL, L_T(r) = LP$	(1) $L_V(LL, j) \neq L_T(LL, j)$ (2) $L_V(r) = LL, L_T(r) = ML$ (3) $L_V(r) = LL, L_T(r) = LR$
	(8) $L_V(r) = LR, L_T(r) = LP$	(1) $L_V(LR, j) \neq L_T(LR, j)$ (2) $L_V(r) = LR, L_T(r) = ML$ (3) $L_V(r) = LR, L_T(r) = LL$
	(9) $L_V(r) = UL, L_T(r) = UP$	(1) $L_V(UL, j) \neq L_T(UL, j)$ (2) $L_V(r) = UL, L_T(r) = MU$ (3) $L_V(r) = UL, L_T(r) = UR$
	(10) $L_V(r) = UR, L_T(r) = UP$	(1) $L_V(UR, j) \neq L_T(UR, j)$ (2) $L_V(r) = UR, L_T(r) = MU$ (3) $L_V(r) = UR, L_T(r) = UL$
	(11) $L_V(r) = ML, L_T(r) \in \{UP, LP\}$	(1) $L_V(r) = ML, L_T(r) = UL$ (2) $L_V(r) = ML, L_T(r) = UR$ (3) $L_V(r) = ML, L_T(r) = LL$ (4) $L_V(r) = ML, L_T(r) = LR$
	(12) $L_V(r) = MU, L_T(r) \in \{UP, LP\}$	(1) $L_V(r) = MU, L_T(r) = UL$ (2) $L_V(r) = MU, L_T(r) = UR$ (3) $L_V(r) = MU, L_T(r) = LL$ (4) $L_V(r) = MU, L_T(r) = LR$
$\mu_{ls}^{'-1}$	(1) $L_T(r) \in \{ML, MU\}$	(1) $L_T(r) = ML$ (2) $L_T(r) = MU$
	(2) $L_T(r) = LL$	(1) $L_T(r) = LL$
	(3) $L_T(r) = LR$	(1) $L_T(r) = LR$
	(4) $L_T(r) = UL$	(1) $L_T(r) = UL$
	(5) $L_T(r) = UR$	(1) $L_T(r) = UR$

Now, we provide the expressions for the occurrence probability of each subscenario in the *ir* service type. For example, $p_{t_{1,1}}$ is the occurrence probability of the first subscenario in scenario 1 ($L_V(r) = ML, L_T(r) = ML$). The probability that the vehicle is located below the cross-aisle as well as in the main aisle is given by $\left(\frac{N_{cl}}{N_c}\right)\left(\frac{1}{N_a}\right)$. Likewise, the probability that the pallet has to be retrieved from a location which is below the cross-aisle as well as in the main aisle is given by $\left(\frac{N_{cl}}{N_c}\right)\left(\frac{1}{N_a}\right)$. Therefore, $p_{t_{1,1}}$ is expressed by $\left(\frac{N_{cl}^2}{N_c^2}\right)\left(\frac{1}{N_a^2}\right)$. By taking a sum of probability of the subscenarios, the probability of the scenario, p_{t_1} can be obtained. We use the relationship, $N_c = N_{cu} + N_{cl}$ and $N_a = N_{ar} + N_{al} + 1$ in simplifying the expressions.

Probability expressions for the subscenarios corresponding to scenario 1.

$$p_{t_{1,1}} = \left(\frac{N_{cl}^2}{N_c^2}\right)\left(\frac{1}{N_a^2}\right)$$

$$p_{t_{1,2}} = \left(\frac{N_{cu}^2}{N_c^2}\right)\left(\frac{1}{N_a^2}\right)$$

$$
\begin{aligned}
p_{t_{1,3}} &= \left(\frac{N_{cl}\times N_{cu}}{N_c^2}\right)\left(\frac{1}{N_a^2}\right)\\
p_{t_{1,4}} &= \left(\frac{N_{cl}\times N_{cu}}{N_c^2}\right)\left(\frac{1}{N_a^2}\right)\\
p_{t_1} &= p_{t_{1,1}} + p_{t_{1,2}} + p_{t_{1,3}} + p_{t_{1,4}}\\
&= \left(\frac{1}{N_c^2N_a^2}\right)\left(N_{cu}^2 + N_{cl}^2 + 2N_{cu}N_{cl}\right)\\
&= \frac{N_c^2}{N_c^2N_a^2} \qquad \text{(C.1)}
\end{aligned}
$$

Probability expressions for the subscenarios corresponding to scenario 2.

$$
\begin{aligned}
p_{t_{2,1}} &= \left(\frac{N_{cu}^2}{N_c^2}\right)\left(\frac{N_{al}}{N_a^2}\right)\\
p_{t_{2,2}} &= \left(\frac{N_{cl}^2}{N_c^2}\right)\left(\frac{N_{al}}{N_a^2}\right)\\
p_{t_{2,3}} &= \left(\frac{N_{cu}^2}{N_c^2}\right)\left(\frac{N_{ar}}{N_a^2}\right)\\
p_{t_{2,4}} &= \left(\frac{N_{cl}^2}{N_c^2}\right)\left(\frac{N_{ar}}{N_a^2}\right)\\
p_{t_2} &= p_{t_{2,1}} + p_{t_{2,2}} + p_{t_{2,3}} + p_{t_{2,4}}\\
&= \frac{(N_a-1)(N_{cu}^2+N_{cl}^2)}{N_c^2N_a^2} \qquad \text{(C.2)}
\end{aligned}
$$

Probability expressions for the subscenarios corresponding to scenario 3.

$$
\begin{aligned}
p_{t_{3,1}} &= \left(\frac{N_{cl}\times N_{cu}}{N_c^2}\right)\left(\frac{N_{al}^2}{N_a^2}\right)\\
p_{t_{3,2}} &= \left(\frac{N_{cl}\times N_{cu}}{N_c^2}\right)\left(\frac{N_{al}}{N_a^2}\right)\\
p_{t_{3,3}} &= \left(\frac{N_{cl}\times N_{cu}}{N_c^2}\right)\left(\frac{N_{al}\times N_{ar}}{N_a^2}\right)\\
p_{t_3} &= p_{t_{3,1}} + p_{t_{3,2}} + p_{t_{3,3}}\\
&= \frac{(N_aN_{al}N_{cl}N_{cu})}{N_c^2N_a^2} \qquad \text{(C.3)}
\end{aligned}
$$

Probability expressions for the subscenarios corresponding to scenario 4.

$$
\begin{aligned}
p_{t_{4,1}} &= \left(\frac{N_{cl}\times N_{cu}}{N_c^2}\right)\left(\frac{N_{ar}^2}{N_a^2}\right)\\
p_{t_{4,2}} &= \left(\frac{N_{cl}\times N_{cu}}{N_c^2}\right)\left(\frac{N_{ar}}{N_a^2}\right)\\
p_{t_{4,3}} &= \left(\frac{N_{cl}\times N_{cu}}{N_c^2}\right)\left(\frac{N_{al}\times N_{ar}}{N_a^2}\right)\\
p_{t_4} &= p_{t_{4,1}} + p_{t_{4,2}} + p_{t_{4,3}}\\
&= \frac{(N_aN_{ar}N_{cl}N_{cu})}{N_c^2N_a^2} \qquad \text{(C.4)}
\end{aligned}
$$

Probability expressions for the subscenarios corresponding to scenario 5.

$$
\begin{aligned}
p_{t_{5,1}} &= \left(\frac{N_{cl}\times N_{cu}}{N_c^2}\right)\left(\frac{N_{al}^2}{N_a^2}\right)\\
p_{t_{5,2}} &= \left(\frac{N_{cl}\times N_{cu}}{N_c^2}\right)\left(\frac{N_{al}}{N_a^2}\right)\\
p_{t_{5,3}} &= \left(\frac{N_{cl}\times N_{cu}}{N_c^2}\right)\left(\frac{N_{al}\times N_{ar}}{N_a^2}\right)\\
p_{t_5} &= p_{t_{5,1}} + p_{t_{5,2}} + p_{t_{5,3}}\\
&= \frac{(N_aN_{al}N_{cl}N_{cu})}{N_c^2N_a^2} \qquad \text{(C.5)}
\end{aligned}
$$

Probability expressions for the subscenarios corresponding to scenario 6.

$$
\begin{aligned}
p_{t_{6,1}} &= \left(\frac{N_{cl}\times N_{cu}}{N_c^2}\right)\left(\frac{N_{ar}^2}{N_a^2}\right)\\
p_{t_{6,2}} &= \left(\frac{N_{cl}\times N_{cu}}{N_c^2}\right)\left(\frac{N_{ar}}{N_a^2}\right)\\
p_{t_{6,3}} &= \left(\frac{N_{cl}\times N_{cu}}{N_c^2}\right)\left(\frac{N_{al}\times N_{ar}}{N_a^2}\right)\\
p_{t_6} &= p_{t_{6,1}} + p_{t_{6,2}} + p_{t_{6,3}}\\
&= \frac{(N_aN_{ar}N_{cl}N_{cu})}{N_c^2N_a^2} \qquad \text{(C.6)}
\end{aligned}
$$

Probability expressions for the subscenarios corresponding to scenario 7.

$$
\begin{aligned}
p_{t_{7,1}} &= \left(\frac{N_{cl}^2}{N_c^2}\right)\left(\frac{N_{al}^2}{N_a^2}\right)\left(\frac{N_{al}-1}{N_{al}}\right)\\
p_{t_{7,2}} &= \left(\frac{N_{cl}^2}{N_c^2}\right)\left(\frac{N_{al}}{N_a^2}\right)\\
p_{t_{7,3}} &= \left(\frac{N_{cl}^2}{N_c^2}\right)\left(\frac{N_{al}\times N_{ar}}{N_a^2}\right)\\
p_{t_7} &= p_{t_{7,1}} + p_{t_{7,2}} + p_{t_{7,3}}\\
&= \frac{(N_{al}^2 + N_{al}N_{ar})N_{cl}^2}{N_c^2N_a^2} \qquad \text{(C.7)}
\end{aligned}
$$

Probability expressions for the subscenarios corresponding to scenario 8.

$$
\begin{aligned}
p_{t_{8,1}} &= \left(\frac{N_{cl}^2}{N_c^2}\right)\left(\frac{N_{ar}^2}{N_a^2}\right)\left(\frac{N_{ar}-1}{N_{ar}}\right)\\
p_{t_{8,2}} &= \left(\frac{N_{cl}^2}{N_c^2}\right)\left(\frac{N_{ar}}{N_a^2}\right)\\
p_{t_{8,3}} &= \left(\frac{N_{cl}^2}{N_c^2}\right)\left(\frac{N_{al}\times N_{ar}}{N_a^2}\right)\\
p_{t_8} &= p_{t_{8,1}} + p_{t_{8,2}} + p_{t_{8,3}}\\
&= \frac{(N_{ar}^2 + N_{al}N_{ar})N_{cl}^2}{N_c^2N_a^2} \qquad \text{(C.8)}
\end{aligned}
$$

Probability expressions for the subscenarios corresponding to scenario 9.

$$
\begin{aligned}
p_{t_{9,1}} &= \left(\frac{N_{cu}^2}{N_c^2}\right)\left(\frac{N_{al}^2}{N_a^2}\right)\left(\frac{N_{al}-1}{N_{al}}\right)\\
p_{t_{9,2}} &= \left(\frac{N_{cu}^2}{N_c^2}\right)\left(\frac{N_{al}}{N_a^2}\right)\\
p_{t_{9,3}} &= \left(\frac{N_{cu}^2}{N_c^2}\right)\left(\frac{N_{al}\times N_{ar}}{N_a^2}\right)\\
p_{t_9} &= p_{t_{9,1}} + p_{t_{9,2}} + p_{t_{9,3}}\\
&= \frac{(N_{al}^2 + N_{al}N_{ar})N_{cu}^2}{N_c^2N_a^2} \qquad \text{(C.9)}
\end{aligned}
$$

Probability expressions for the subscenarios corresponding to scenario 10.

$$
\begin{aligned}
p_{t_{10,1}} &= \left(\frac{N_{cu}^2}{N_c^2}\right)\left(\frac{N_{ar}^2}{N_a^2}\right)\left(\frac{N_{ar}-1}{N_{ar}}\right)\\
p_{t_{10,2}} &= \left(\frac{N_{cu}^2}{N_c^2}\right)\left(\frac{N_{ar}}{N_a^2}\right)
\end{aligned}
$$

Table C.2
Expressions for service time (excluding load/unload times) for different scenarios with change in cross-aisle location.

Expected service time	Term	Expression
$\mu_{ir}'^{-1}$	$t_{1,1}$	$\left(\frac{N_{cl}^2}{N_c^2}\right)\left(\frac{1}{N_a^2}\right)\left(\frac{W_l}{3v_h}+\frac{W_l}{2v_h}\right)$
	$t_{1,2}$	$\left(\frac{N_{cu}^2}{N_c^2}\right)\left(\frac{1}{N_a^2}\right)\left(\frac{W_u}{3v_h}+\frac{W_u}{2v_h}+\frac{W_l}{v_h}+\frac{2x'_w}{v_h}\right)$
	$t_{1,3}$	$\left(\frac{N_{cl}\times N_{cu}}{N_c^2}\right)\left(\frac{1}{N_a^2}\right)\left(\frac{W_u}{2v_h}+\frac{W_l}{v_h}+\frac{2x'_w}{v_h}\right)$
	$t_{1,4}$	$\left(\frac{N_{cl}\times N_{cu}}{N_c^2}\right)\left(\frac{1}{N_a^2}\right)\left(\frac{W_l}{2v_h}+\frac{W_u}{v_h}+\frac{W_l}{v_h}+\frac{4x'_w}{v_h}\right)$
	$t_{2,1}$	$\left(\frac{N_{cu}^2}{N_c^2}\right)\left(\frac{N_{al}}{N_a^2}\right)\left(\frac{W_u}{3v_h}+\frac{W_u}{2v_h}+\frac{2u_d+w_a}{v_h}+\frac{D_l-2u_d-w_a}{2v_h}+\frac{W_l}{v_h}+\frac{2x'_w}{v_h}\right)$
	$t_{2,2}$	$\left(\frac{N_{cl}^2}{N_c^2}\right)\left(\frac{N_{al}}{N_a^2}\right)\left(\frac{W_l}{3v_h}+\frac{W_l}{2v_h}+\frac{2u_d+w_a}{v_h}+\frac{D_l-2u_d-w_a}{2v_h}+\frac{W_l}{v_h}+\frac{2x'_w}{v_h}\right)$
	$t_{2,3}$	$\left(\frac{N_{cu}^2}{N_c^2}\right)\left(\frac{N_{ar}}{N_a^2}\right)\left(\frac{W_u}{3v_h}+\frac{W_u}{2v_h}+\frac{2u_d+w_a}{v_h}+\frac{D_r-2u_d-w_a}{2v_h}+\frac{W_l}{v_h}+\frac{2x'_w}{v_h}\right)$
	$t_{2,4}$	$\left(\frac{N_{cl}^2}{N_c^2}\right)\left(\frac{N_{ar}}{N_a^2}\right)\left(\frac{W_l}{3v_h}+\frac{W_l}{2v_h}+\frac{2u_d+w_a}{v_h}+\frac{D_r-2u_d-w_a}{2v_h}+\frac{W_l}{v_h}+\frac{2x'_w}{v_h}\right)$
	$t_{3,1}$	$\left(\frac{N_{cl}\times N_{cu}}{N_c^2}\right)\left(\frac{N_{al}^2}{N_a^2}\right)\left(\frac{D_l-2u_d-w_a}{3v_h}+\frac{W_l}{v_h}+\frac{W_u}{2v_h}+\frac{D_l-2u_d-w_a}{2v_h}+\frac{2u_d+w_a}{v_h}+\frac{W_l}{v_h}+\frac{4x'_w}{v_h}\right)$
	$t_{3,2}$	$\left(\frac{N_{cl}\times N_{cu}}{N_c^2}\right)\left(\frac{N_{al}}{N_a^2}\right)\left(\frac{D_l-2u_d-w_a}{2v_h}+\frac{2u_d+w_a}{v_h}+\frac{W_l}{v_h}+\frac{2x'_w}{v_h}+\frac{W_u}{2v_h}\right)$
	$t_{3,3}$	$\left(\frac{N_{cl}\times N_{cu}}{N_c^2}\right)\left(\frac{N_{al}\times N_{ar}}{N_a^2}\right)\left(\frac{D_l-2u_d-w_a}{2v_h}+\frac{3(2u_d+w_a)}{v_h}+\frac{2(D_r-2u_d-w_a)}{2v_h}+\frac{W_l}{v_h}+\frac{W_u}{2v_h}+\frac{W_l}{v_h}+\frac{4x'_w}{v_h}\right)$
	$t_{4,1}$	$\left(\frac{N_{cl}\times N_{cu}}{N_c^2}\right)\left(\frac{N_{ar}^2}{N_a^2}\right)\left(\frac{D_r-2u_d-w_a}{3v_h}+\frac{W_l}{v_h}+\frac{D_r-2u_d-w_a}{2v_h}+\frac{2u_d+w_a}{v_h}+\frac{W_l}{v_h}+\frac{4x'_w}{v_h}+\frac{W_u}{2v_h}\right)$
	$t_{4,2}$	$\left(\frac{N_{cl}\times N_{cu}}{N_c^2}\right)\left(\frac{N_{ar}}{N_a^2}\right)\left(\frac{D_r-2u_d-w_a}{2v_h}+\frac{2u_d+w_a}{v_h}+\frac{W_l}{v_h}+\frac{2x'_w}{v_h}+\frac{W_u}{2v_h}\right)$
	$t_{4,3}$	$\left(\frac{N_{cl}\times N_{cu}}{N_c^2}\right)\left(\frac{N_{al}\times N_{ar}}{N_a^2}\right)\left(\frac{D_r-2u_d-w_a}{2v_h}+\frac{3(2u_d+w_a)}{v_h}+\frac{2(D_l-2u_d-w_a)}{2v_h}+\frac{W_l}{v_h}+\frac{W_l}{v_h}+\frac{4x'_w}{v_h}+\frac{W_u}{2v_h}\right)$
	$t_{5,1}$	$\left(\frac{N_{cl}\times N_{cu}}{N_c^2}\right)\left(\frac{N_{al}^2}{N_a^2}\right)\left(\frac{D_l-2u_d-w_a}{3v_h}+\frac{W_u}{v_h}+\frac{D_l-2u_d-w_a}{2v_h}+\frac{2u_d+w_a}{v_h}+\frac{W_l}{v_h}+\frac{4x'_w}{v_h}+\frac{W_l}{2v_h}\right)$
	$t_{5,2}$	$\left(\frac{N_{cl}\times N_{cu}}{N_c^2}\right)\left(\frac{N_{al}}{N_a^2}\right)\left(\frac{D_l-2u_d-w_a}{2v_h}+\frac{2u_d+w_a}{v_h}+\frac{W_u}{v_h}+\frac{4x'_w}{v_h}+\frac{W_l}{2v_h}+\frac{W_l}{v_h}\right)$
	$t_{5,3}$	$\left(\frac{N_{cl}\times N_{cu}}{N_c^2}\right)\left(\frac{N_{al}\times N_{ar}}{N_a^2}\right)\left(\frac{D_l-2u_d-w_a}{2v_h}+\frac{3(2u_d+w_a)}{v_h}+\frac{2(D_r-2u_d-w_a)}{2v_h}+\frac{W_l}{v_h}+\frac{W_u}{2v_h}+\frac{4x'_w}{v_h}+\frac{W_l}{2v_h}\right)$
	$t_{6,1}$	$\left(\frac{N_{cl}\times N_{cu}}{N_c^2}\right)\left(\frac{N_{ar}^2}{N_a^2}\right)\left(\frac{D_r-2u_d-w_a}{3v_h}+\frac{W_l}{2v_h}+\frac{D_r-2u_d-w_a}{2v_h}+\frac{2u_d+w_a}{v_h}+\frac{W_l}{v_h}+\frac{4x'_w}{v_h}+\frac{W_u}{v_h}\right)$
	$t_{6,2}$	$\left(\frac{N_{cl}\times N_{cu}}{N_c^2}\right)\left(\frac{N_{ar}}{N_a^2}\right)\left(\frac{D_r-2u_d-w_a}{2v_h}+\frac{2u_d+w_a}{v_h}+\frac{W_l}{v_h}+\frac{4x'_w}{v_h}+\frac{W_l}{2v_h}+\frac{W_u}{v_h}\right)$
	$t_{6,3}$	$\left(\frac{N_{cl}\times N_{cu}}{N_c^2}\right)\left(\frac{N_{al}\times N_{ar}}{N_a^2}\right)\left(\frac{D_r-2u_d-w_a}{2v_h}+\frac{3(2u_d+w_a)}{v_h}+\frac{2(D_l-2u_d-w_a)}{2v_h}+\frac{W_l}{v_h}+\frac{W_u}{v_h}+\frac{4x'_w}{v_h}+\frac{W_l}{2v_h}\right)$
	$t_{7,1}$	$\left(\frac{N_{cl}^2}{N_c^2}\right)\left(\frac{N_{al}^2}{N_a^2}\right)\left(\frac{N_{al}-1}{N_{al}}\right)\left(\frac{W_l}{2v_h}+\frac{D_l-2u_d-w_a}{3v_h}+\frac{W_l}{v_h}+\frac{D_l-2u_d-w_a}{2v_h}+\frac{W_l}{v_h}+\frac{2u_d+w_a}{v_h}+\frac{4x'_w}{v_h}\right)$
	$t_{7,2}$	$\left(\frac{N_{cl}^2}{N_c^2}\right)\left(\frac{N_{al}}{N_a^2}\right)\left(\frac{W_l}{2v_h}+\frac{D_l-2u_d-w_a}{2v_h}+\frac{2u_d+w_a}{v_h}+\frac{W_l}{v_h}+\frac{2x'_w}{v_h}\right)$
	$t_{7,3}$	$\left(\frac{N_{cl}^2}{N_c^2}\right)\left(\frac{N_{al}\times N_{ar}}{N_a^2}\right)\left(\frac{W_l}{2v_h}+\frac{D_l-2u_d-w_a}{2v_h}+\frac{3(2u_d+w_a)}{v_h}+\frac{2(D_r-2u_d-w_a)}{2v_h}+\frac{W_l}{v_h}+\frac{W_l}{v_h}+\frac{4x'_w}{v_h}\right)$
	$t_{8,1}$	$\left(\frac{N_{cl}^2}{N_c^2}\right)\left(\frac{N_{ar}^2}{N_a^2}\right)\left(\frac{N_{ar}-1}{N_{ar}}\right)\left(\frac{W_l}{2v_h}+\frac{D_r-2u_d-w_a}{3v_h}+\frac{W_l}{v_h}+\frac{D_r-2u_d-w_a}{2v_h}+\frac{W_l}{v_h}+\frac{2u_d+w_a}{v_h}+\frac{4x'_w}{v_h}\right)$
	$t_{8,2}$	$\left(\frac{N_{cl}^2}{N_c^2}\right)\left(\frac{N_{ar}}{N_a^2}\right)\left(\frac{W_l}{2v_h}+\frac{D_r-2u_d-w_a}{2v_h}+\frac{2u_d+w_a}{v_h}+\frac{W_l}{v_h}+\frac{2x'_w}{v_h}\right)$
	$t_{8,3}$	$\left(\frac{N_{cl}^2}{N_c^2}\right)\left(\frac{N_{al}\times N_{ar}}{N_a^2}\right)\left(\frac{W_l}{2v_h}+\frac{D_r-2u_d-w_a}{2v_h}+\frac{3(2u_d+w_a)}{v_h}+\frac{2(D_l-2u_d-w_a)}{2v_h}+\frac{W_l}{v_h}+\frac{W_l}{v_h}+\frac{4x'_w}{v_h}\right)$
$\mu_{ir}'^{-1}$	$t_{9,1}$	$\left(\frac{N_{cu}^2}{N_c^2}\right)\left(\frac{N_{al}^2}{N_a^2}\right)\left(\frac{N_{al}-1}{N_{al}}\right)\left(\frac{W_u}{2v_h}+\frac{D_l-2u_d-w_a}{3v_h}+\frac{W_u}{v_h}+\frac{D_l-2u_d-w_a}{2v_h}+\frac{W_l}{v_h}+\frac{2u_d+w_a}{v_h}+\frac{4x'_w}{v_h}\right)$
	$t_{9,2}$	$\left(\frac{N_{cu}^2}{N_c^2}\right)\left(\frac{N_{al}}{N_a^2}\right)\left(\frac{W_u}{2v_h}+\frac{D_l-2u_d-w_a}{2v_h}+\frac{2u_d+w_a}{v_h}+\frac{W_l+W_u}{v_h}+\frac{4x'_w}{v_h}\right)$
	$t_{9,3}$	$\left(\frac{N_{cu}^2}{N_c^2}\right)\left(\frac{N_{al}\times N_{ar}}{N_a^2}\right)\left(\frac{W_u}{2v_h}+\frac{D_l-2u_d-w_a}{2v_h}+\frac{3(2u_d+w_a)}{v_h}+\frac{2(D_r-2u_d-w_a)}{2v_h}+\frac{W_u}{v_h}+\frac{W_l}{v_h}+\frac{4x'_w}{v_h}\right)$
	$t_{10,1}$	$\left(\frac{N_{cu}^2}{N_c^2}\right)\left(\frac{N_{ar}^2}{N_a^2}\right)\left(\frac{N_{ar}-1}{N_{ar}}\right)\left(\frac{W_u}{2v_h}+\frac{D_r-2u_d-w_a}{3v_h}+\frac{W_l}{v_h}+\frac{D_r-2u_d-w_a}{2v_h}+\frac{W_u}{v_h}+\frac{2u_d+w_a}{v_h}+\frac{4x'_w}{v_h}\right)$
	$t_{10,2}$	$\left(\frac{N_{cu}^2}{N_c^2}\right)\left(\frac{N_{ar}}{N_a^2}\right)\left(\frac{W_l}{2v_h}+\frac{D_r-2u_d-w_a}{2v_h}+\frac{2u_d+w_a}{v_h}+\frac{W_l}{v_h}+\frac{2x'_w}{v_h}\right)$
	$t_{10,3}$	$\left(\frac{N_{cu}^2}{N_c^2}\right)\left(\frac{N_{al}\times N_{ar}}{N_a^2}\right)\left(\frac{W_u}{2v_h}+\frac{D_r-2u_d-w_a}{2v_h}+\frac{3(2u_d+w_a)}{v_h}+\frac{2(D_l-2u_d-w_a)}{2v_h}+\frac{W_u}{v_h}+\frac{W_l}{v_h}+\frac{4x'_w}{v_h}\right)$
	$t_{11,1}$	$\left(\frac{N_{cl}\times N_{cu}}{N_c^2}\right)\left(\frac{N_{al}}{N_a^2}\right)\left(\frac{2(2u_d+w_a)}{v_h}+\frac{2(D_l-2u_d-w_a)}{2v_h}+\frac{W_u}{v_h}+\frac{W_l}{v_h}+\frac{W_l}{2v_h}+\frac{4x'_w}{v_h}\right)$
	$t_{11,2}$	$\left(\frac{N_{cl}\times N_{cu}}{N_c^2}\right)\left(\frac{N_{ar}}{N_a^2}\right)\left(\frac{2(2u_d+w_a)}{v_h}+\frac{2(D_r-2u_d-w_a)}{2v_h}+\frac{W_u}{v_h}+\frac{W_l}{v_h}+\frac{W_l}{2v_h}+\frac{4x'_w}{v_h}\right)$
	$t_{11,3}$	$\left(\frac{N_{cl}^2}{N_c^2}\right)\left(\frac{N_{al}}{N_a^2}\right)\left(\frac{2(2u_d+w_a)}{v_h}+\frac{2(D_l-2u_d-w_a)}{2v_h}+\frac{2W_l}{v_h}+\frac{W_l}{2v_h}+\frac{4x'_w}{v_h}\right)$
	$t_{11,4}$	$\left(\frac{N_{cl}^2}{N_c^2}\right)\left(\frac{N_{ar}}{N_a^2}\right)\left(\frac{2(2u_d+w_a)}{v_h}+\frac{2(D_r-2u_d-w_a)}{2v_h}+\frac{2W_l}{v_h}+\frac{W_l}{2v_h}+\frac{4x'_w}{v_h}\right)$
	$t_{12,1}$	$\left(\frac{N_{cu}^2}{N_c^2}\right)\left(\frac{N_{al}}{N_a^2}\right)\left(\frac{2(2u_d+w_a)}{v_h}+\frac{2(D_l-2u_d-w_a)}{2v_h}+\frac{W_u}{v_h}+\frac{W_l}{v_h}+\frac{W_u}{2v_h}+\frac{4x'_w}{v_h}\right)$
	$t_{12,2}$	$\left(\frac{N_{cu}^2}{N_c^2}\right)\left(\frac{N_{ar}}{N_a^2}\right)\left(\frac{2(2u_d+w_a)}{v_h}+\frac{2(D_r-2u_d-w_a)}{2v_h}+\frac{W_u}{v_h}+\frac{W_l}{v_h}+\frac{W_u}{2v_h}+\frac{4x'_w}{v_h}\right)$
	$t_{12,3}$	$\left(\frac{N_{cu}\times N_{cl}}{N_c^2}\right)\left(\frac{N_{al}}{N_a^2}\right)\left(\frac{2(2u_d+w_a)}{v_h}+\frac{2(D_l-2u_d-w_a)}{2v_h}+\frac{2W_l}{v_h}+\frac{W_u}{2v_h}+\frac{4x'_w}{v_h}\right)$
	$t_{12,4}$	$\left(\frac{N_{cu}\times N_{cl}}{N_c^2}\right)\left(\frac{N_{ar}}{N_a^2}\right)\left(\frac{2(2u_d+w_a)}{v_h}+\frac{2(D_r-2u_d-w_a)}{2v_h}+\frac{2W_l}{v_h}+\frac{W_u}{2v_h}+\frac{4x'_w}{v_h}\right)$
$\mu_{ls}'^{-1}$	$u_{1,1}$	$\left(\frac{N_{cl}}{N_c}\right)\left(\frac{1}{N_a}\right)\left(\frac{W_l}{2v_h}\right)$
	$u_{1,2}$	$\left(\frac{N_{cu}}{N_c}\right)\left(\frac{1}{N_a}\right)\left(\frac{W_l}{v_h}+\frac{W_u}{2v_h}+\frac{2x'_w}{v_h}\right)$
	$u_{2,1}$	$\left(\frac{N_{cl}}{N_c}\right)\left(\frac{N_{al}}{N_a}\right)\left(\frac{W_l}{v_h}+\frac{(2u_d+w_a)}{v_h}+\frac{D_l-2u_d-w_a}{2v_h}+\frac{2x'_w}{v_h}+\frac{W_l}{2v_h}\right)$
	$u_{3,1}$	$\left(\frac{N_{cu}}{N_c}\right)\left(\frac{N_{ar}}{N_a}\right)\left(\frac{W_l}{v_h}+\frac{(2u_d+w_a)}{v_h}+\frac{D_l-2u_d-w_a}{2v_h}+\frac{2x'_w}{v_h}+\frac{W_u}{2v_h}\right)$
	$u_{4,1}$	$\left(\frac{N_{cl}}{N_c}\right)\left(\frac{N_{al}}{N_a}\right)\left(\frac{W_l}{v_h}+\frac{(2u_d+w_a)}{v_h}+\frac{D_r-2u_d-w_a}{2v_h}+\frac{2x'_w}{v_h}+\frac{W_l}{2v_h}\right)$
	$u_{5,1}$	$\left(\frac{N_{cu}}{N_c}\right)\left(\frac{N_{ar}}{N_a}\right)\left(\frac{W_l}{v_h}+\frac{(2u_d+w_a)}{v_h}+\frac{D_r-2u_d-w_a}{2v_h}+\frac{2x'_w}{v_h}+\frac{W_u}{2v_h}\right)$

$$p_{t_{10,3}} = \left(\frac{N_{cu}^2}{N_c^2}\right)\left(\frac{N_{al}\times N_{ar}}{N_a^2}\right)$$

$$p_{t_{10}} = p_{t_{10,1}} + p_{t_{10,2}} + p_{t_{10,3}} = \frac{(N_{ar}^2 + N_{al}N_{ar})N_{cu}^2}{N_c^2 N_a^2} \tag{C.10}$$

Probability expressions for the subscenarios corresponding to scenario 11.

$$p_{t_{11,1}} = \left(\frac{N_{cl}\times N_{cu}}{N_c^2}\right)\left(\frac{N_{al}}{N_a^2}\right)$$

$$p_{t_{11,2}} = \left(\frac{N_{cl}\times N_{cu}}{N_c^2}\right)\left(\frac{N_{ar}}{N_a^2}\right)$$

Table C.3
Service time expressions for variations in cross-aisle location.

Expected service time	Expression
$\mu_{ir}^{'-1}$	$\sum_{m=1}^{12}\sum_{n=1}^{N_s(m)} t_{m,n} + L_{vt} + U_{vt}$
$\mu_{ls}^{'-1}$	$\sum_{m=1}^{5}\sum_{n=1}^{N_s(m)} u_{m,n} + L_{vt} + U_{vt}$
$\mu_{lr}^{'-1}$	$2\sum_{m=1}^{5}\sum_{n=1}^{N_s(m)} u_{m,n} + L_{vt} + U_{vt}$
$\mu_{is}^{'-1}$	$2\sum_{m=1}^{5}\sum_{n=1}^{N_s(m)} u_{m,n} + L_{vt} + U_{vt}$
μ_{ex}^{-1}	$\sum_{m=1}^{5}\sum_{n=1}^{N_s(m)} u_{m,n}$

$$p_{t_{11,3}} = \left(\frac{N_{cl}^2}{N_c^2}\right)\left(\frac{N_{al}}{N_a^2}\right)$$

$$p_{t_{11,4}} = \left(\frac{N_{cl}^2}{N_c^2}\right)\left(\frac{N_{ar}}{N_a^2}\right)$$

$$\begin{aligned} p_{t_{11}} &= p_{t_{11,1}} + p_{t_{11,2}} + p_{t_{11,3}} + p_{t_{11,4}} \\ &= \left(\frac{(N_a-1)(N_{cl}\times N_{cu} + N_{cl}^2)}{N_c^2 N_a^2}\right) \end{aligned} \tag{C.11}$$

Probability expressions for the subscenarios corresponding to scenario 12.

$$p_{t_{12,1}} = \left(\frac{N_{cu}^2}{N_c^2}\right)\left(\frac{N_{al}}{N_a^2}\right)$$

$$p_{t_{12,2}} = \left(\frac{N_{cu}^2}{N_c^2}\right)\left(\frac{N_{ar}}{N_a^2}\right)$$

$$p_{t_{12,3}} = \left(\frac{N_{cu}\times N_{cl}}{N_c^2}\right)\left(\frac{N_{al}}{N_a^2}\right)$$

$$p_{t_{12,4}} = \left(\frac{N_{cu}\times N_{cl}}{N_c^2}\right)\left(\frac{N_{ar}}{N_a^2}\right)$$

$$\begin{aligned} p_{t_{12}} &= p_{t_{12,1}} + p_{t_{12,2}} + p_{t_{12,3}} + p_{t_{12,4}} \\ &= \left(\frac{(N_a-1)(N_{cl}\times N_{cu} + N_{cu}^2)}{N_c^2 N_a^2}\right) \end{aligned} \tag{C.12}$$

The sum of the probabilities across all scenarios for the *ir* service type, p_{t_i}, where $i = 1, \ldots, 12$, is unity. Now, we provide the expressions for the occurrence probability of each subscenario in the *ls* service type. For example, $p_{u_{1,1}}$ is the occurrence probability of the first subscenario in scenario 1. $L_V(r)$ is LU point, $L_T(r) = ML$. The probability that the transaction is located below the cross-aisle and is present in the main aisle is given by $\left(\frac{N_{cl}}{N_c}\right)\left(\frac{1}{N_a}\right)$. Likewise, the occurrence probabilities for the remaining five subscenarios are included below.

$$p_{u_{1,1}} = \left(\frac{N_{cl}}{N_c}\right)\left(\frac{1}{N_a}\right) \tag{C.13}$$

$$p_{u_{1,2}} = \left(\frac{N_{cu}}{N_c}\right)\left(\frac{1}{N_a}\right) \tag{C.14}$$

$$p_{u_{2,1}} = \left(\frac{N_{cl}}{N_c}\right)\left(\frac{N_{al}}{N_a}\right) \tag{C.15}$$

$$p_{u_{3,1}} = \left(\frac{N_{cu}}{N_c}\right)\left(\frac{N_{ar}}{N_a}\right) \tag{C.16}$$

$$p_{u_{4,1}} = \left(\frac{N_{cl}}{N_c}\right)\left(\frac{N_{al}}{N_a}\right) \tag{C.17}$$

$$p_{u_{5,1}} = \left(\frac{N_{cu}}{N_c}\right)\left(\frac{N_{ar}}{N_a}\right) \tag{C.18}$$

Now, we provide the expressions for unconditional expected travel times in each subscenario (for *ir* service type). Note that the expected travel time in each subscenario is conditional on the location of the vehicle and the transaction. Hence, we uncondition the expected travel times by multiplying the conditional travel times with the subscenario probabilities provided by Eqs. (C.1)–(C.12).

The expected travel time for the first subscenario, $L_V(r) = ML, L_T(r) = ML$ is obtained as follows (refer Fig. 6). Since the vehicle is in the lower portion of the cross-aisle, the expected travel time to reach the retrieval location from its dwell-point is given by $\frac{W_l}{3v_h}$. Then the vehicle picks the pallet and moves towards the LU point. This travel time is given by $\frac{W_l}{2v_h}$. Hence, the unconditional expected travel time is given by the total travel time multiplied by the subscenario probability, which is $\left(\frac{N_{cl}^2}{N_c^2}\right)\left(\frac{1}{N_a^2}\right)\left(\frac{W_l}{3v_h} + \frac{W_l}{2v_h}\right)$. For the second subscenario, $L_V(r) = MU, L_T(r) = MU$, first the vehicle travels from its dwell-point to the retrieval location, and then reaches the cross-aisle, travels the X-way distance, and proceeds towards the LU point using the main aisle, which is given by $\left(\frac{N_{cu}^2}{N_c^2}\right)\left(\frac{1}{N_a^2}\right)\left(\frac{W_u}{3v_h} + \frac{W_u}{2v_h} + \frac{W_l}{v_h} + \frac{2x'_w}{v_h}\right)$. Using a similar approach, we now explain the expression for the third subscenario of scenario 3, which has more number of travel movements. In this case, $L_V(r) = UL, L_T(r) = LR$, therefore the vehicle is in the upper left zone and the pallet needs to be retrieved from the lower right zone. Note that some travel time components are deterministic, whereas some travel time components are stochastic. The expected cross-aisle and aisle travel in the UL zone are given by $\frac{W_u}{2v_h}$ and $\frac{D_l - 2u_d - w_a}{2v_h}$ respectively. Likewise, the expected cross-aisle and aisle travel in the LR zone are given by $\frac{2(D_r - 2u_d - w_a)}{2v_h} + \frac{W_l}{v_h} + \frac{W_l}{v_h}$. The deterministic travel time between the UL and the LR zone along the cross-aisle is given by $\frac{3(2u_d + w_a)}{v_h}$. The deterministic travel along the X-way is given by $\frac{4x'_w}{h}$. The probability for this subscenario $(\frac{N_{cl}\times N_{cu}}{N_c^2})$ is multiplied with the conditional total expected travel time for this subscenario to determine the unconditional travel time. We use similar methodology for calculating the probability weighted travel times for the remaining subscenarios (see Table C.2).

References

Baskett, F., Chandy, K., Muntz, R., & Palacios, F. (1975). Open, closed and mixed networks of queues with different classes of customers. *Journal of the ACM*, *22*, 248–260.

Berglund, P., & Batta, R. (2012). Optimal placement of warehouse cross-aisles in a picker-to-part warehouse with class-based storage. *IIE Transactions*, *44*(2), 107–120.

Bolch, G., Stefan, G., Meer, H., & Trivedi, K. (2006). *Queueing networks and Markov chains: Modeling and performance evaluation with computer science applications* (vol. 2). Hoboken, New Jersey: John Wiley and Sons.

Buzen, J. (1973). Computational algorithms for closed queueing networks with exponential servers. *Communications of the ACM*, *16*(3), 527–531.

Ekren, B. Y., Heragu, S. S., Krishnamurthy, A., & Malmborg, C. J. (2010). Simulation based experimental design to identify factors affecting performance of AVS/RS. *Computers & Industrial Engineering*, *58*(1), 175–185.

Ertek, G., Incel, B., & Arslan, M. C. (2007). Impact of cross aisles in a rectangular warehouse: A computational study. In M. Lahmar (Ed.), *Facility logistics: Approaches and solutions to next generation challenges* (pp. 97–125). Auerbach Publications.

Fukunari, M., & Malmborg, C. (2009). A network queuing approach for evaluation of performance measures in autonomous vehicle storage and retrieval systems. *European Journal of Operational Research*, *193*, 152–167.

Gross, D., Shortle, J. F., Thompson, J. M., & Harris, C. M. (2008). *Fundamentals of queueing theory* (vol. 4). Hoboken, New Jersey: John Wiley and Sons.

Heragu, S., Cai, X., Krishnamurthy, A., & Malmborg, C. (2008). Striving for warehouse excellence. *Industrial Engineer*, *40*(12), 43–47.

Kuo, P., Krishnamurthy, A., & Malmborg, C. (2007). Design models for unit load storage and retrieval systems using autonomous vehicle technology and resource conserving storage and dwell point policies. *Applied Mathematical Modelling*, *31*, 2332–2346.

Malmborg, C. (2002). Conceptualizing tools for autonomous vehicle storage and retrieval systems. *International Journal of Production Research*, *40*(8), 1807–1822.

Malmborg, C. (2003). Interleaving dynamics in autonomous vehicle storage and retrieval systems. *International Journal of Production Research*, *41*(5), 1057–1069.

Meller, R., & Mungwattana, A. (2005). AS/RS dwell-point strategy selection at high system utilization: A simulation study to investigate the magnitude of the benefit. *International Journal of Production Research*, *43*(24), 5217–5227.

Öztürkoglu, O., Gue, K. R., & Meller, R. D. (2012). Optimal unit-load warehouse designs for single-command operations. *IIE Transactions*, *44*(6), 459–475.

Park, B. C. (1999). Optimal dwell point policies for automated storage/retrieval systems with dedicated storage. *IIE Transactions*, *31*(10), 1011–1113.

Reiser, M., & Lavenberg, S. S. (1980). Mean-value analysis of closed multichain queuing networks. *Journal of the ACM*, *27*(2), 313–322.

Roodbergen, K.-J., & De Koster, R. (2001). Routing order pickers in a warehouse with a middle aisle. *European Journal of Operational Research*, *133*, 32–43.

Roy, D. (2011). *Design and analysis of unit-load warehouse operations using autonomous vehicles* (Ph.D. thesis). Madison, Wisconsin: Department of Industrial and Systems Engineering, University of Wisconsin-Madison.

Roy, D., Krishnamurthy, A., Heragu, S., & Malmborg, C. (2012). Performance analysis and design trade-offs in warehouses with autonomous vehicle technology. *IIE Transactions*, *44*(12) 1045–1060.

van den Berg, J. (2002). Analytic expressions for the optimal dwell point in an automated storage/retrieval system. *International Journal of Production Economics*, *72*(1), 13–25.

Vaughan, T. S., & Petersen, C. (1999). The effect of warehouse cross aisles on order picking efficiency. *International Journal of Production Research*, *37*(4), 881–897.

Ventura, J. A., & Lee, C. (2003). Optimally locating multiple dwell points in a single loop guide path system. *IIE Transactions*, *35*(8), 727–737.

Zhang, L. (2008). *Methodological foundations for design conceptualization of autonomous vehicle storage and retrieval systems*. (Ph.D. thesis). Department of Decision Sciences and Engineering Systems, Rensselaer Polytechnic Institute Troy, New York.

Zhang, L., Krishnamurthy, A., Malmborg, C., & Heragu, S. (2009). Variance-based approximations of transaction waiting times in autonomous vehicle storage and retrieval systems. *European Journal of Industrial Engineering*, *3*(2), 146–169.